NTNU – Trondheim
Norwegian University of
Science and Technology

Synthetic Inertia from Wind Farms - Impacts on Rotor Angle Stability in Existing Synchronous Generators

Amund Strømnes
Øverjordet

Master of Energy and Environmental Engineering
Submission date: June 2014
Supervisor: Kjetil Uhlen, ELKRAFT

Norwegian University of Science and Technology
Department of Electric Power Engineering

Abstract

As the share of wind power in the power system rises, synchronous generators in traditional power plants are taken out of the grid and replaced by a large number of wind turbines. Most modern wind turbines utilize a power electronic interface between the generator and grid to allow variable speed operation of the turbine. By introducing the power electronic interface the wind turbine do not contribute to the rotational mass of the system or the frequency control. When the share of wind power becomes significant, the primary frequency response is influenced and the activation of primary reserves are challenged. To meet the demand for contribution to rotating mass, synthetic inertia emulation is proposed as a solution.

There are numerous studies showing that synthetic inertia provides an important response from a frequency stability point of view. However, these models utilize weak representations of the grid, losing information about rotor angle stability. In this thesis a higher order simulation model is built in Simulink/Matlab to evaluate impacts on rotor angle stability from utilization of synthetic inertia. The main conclusions from the performed simulations are that the phase of the inertial response determines if the system damping is reduced, and that the inertia emulation should counteract frequency changes, not deviations. Also it is shown that the aggressiveness of the inverter tuning largely influences the damping of the oscillations in the system. However, a controller tuning is found where the system damping is acceptable and the inertial contribution from the wind farm is significant.

Sammendrag

Når andelen vindkraft i kraftsystemet øker, endres systemets sammensetning av generatorer. Tradisjonelle synkrongeneratorer fases ut og blir erstattet med et større antall vindturbiner. Så godt som alle moderne vindturbiner benytter et ledd bestående av kraftelektronikk mellom turbinens generator og nettet, dette for å tillate variabel hastighet på turbinen. Ved å introdusere kraftelektronikk mellom generator og nett bidrar ikke lengre turbinen til nettets roterende masse. Ettersom andelen vindkraft i systemet øker vil dette påvirke nettets frekvensrespons ved å tillate hurtigere frekvensendringer. Dette vil gjøre primærreguleringen i nettet mer utfordrende. For å møte etterspørselen etter bidrag til roterende masse er syntetisk treghet foreslått som løsning.

Det finnes mange studier som viser at syntetisk treghet gir et viktig bidrag for å beholde frekvensstabiliteten i systemet når store menger vindkraft fases inn. De fleste av disse studiene benytter seg derimot av modeller med en svak representasjon av nettet, som ikke inneholder informasjon om vinkelstabilitet i synkrongeneratorer. I denne oppgaven er det bygget en høyere ordens simuleringsmodell i Simulink/Matlab for å evaluere hvordan vinkelstabilitet i synkrongeneratorer påvirkes av syntetisk treghet i vindturbiner. Konklusjonene trukket fra simuleringene er at fasen til response fra den syntetiske tregheten avgjør om dempingen av systems svingninger reduseres. Det virker hensiktsmessig at tregheten skal motvirke endringer i frekvens, ikke avvik i frekvens. Det er også observert at stivheten til omformeren har overraskende stor påvirkning på dempingen av svingningene i systemet. Det ble funnet kontrollparametre som både gav akseptabel demping av svingningene i systemet og et vesentlig bidrag til roterende masse i systemet.

Acknowledgments

I would like to thank professor Kjetil Uhlen at the Department of Electric Power Engineering at NTNU for all help, motivation and guidance. Also I would like to thank Dr. Olimpo Anaya-Lara at the University of Strathclyde for your advice.

Contents

1 Introduction

1.1 Motivation

Recently changes have been introduced to the European power system. Political initiatives are taken to replace traditional thermal power plants with renewable energy sources, both to reduce greenhouse gas emissions and reduce the dependance on nuclear power plants. To increase the share of renewable energy in the power system, increasing amounts of wind power are introduced to the power system. As the new renewable energy sources are phased into the power system several challenges rise for the transmission system operators. The new energy sources utilize new generator solutions with power electronic interfaces between the grid and the generator. The power electronic interface decouple the generator from the rest of the grid giving no contribution to the system inertia.

When the penetration of new renewable energy sources becomes significant the lack of inertial contribution will affect the dynamic performance of the entire power system. As the share of wind power and other renewable energy sources increases, it is expected that these will contribute to the system frequency control by providing synthetic inertia by inertia emulation [1]. This has been shown to be an efficient way to improve the frequency stability in the system. However, impacts from inertia emulation on transient stability in the system have been given little attention.

During the specialization project regarding frequency stability and synthetic inertia, it was noticed that the response from the wind farm was close to a step increase in power output. To investigate how this rapid increase affects the stability of synchronous generators is the basis for this master thesis. The goal is to investigate how the inertia emulation in wind farms affects the damping of the electromechanical oscillations in other synchronous generators in the system. Impacts on the transient stability of the system, through studies of critical clearing time, and how power oscillations between areas may be affected will also be studied.

1.2 Method

The method will be to build a simulation model in the MATLAB based Simulink workspace. The aim will be to model the dynamic behavior of synchronous generators using the same approach as traditional power system analysis software. The model will also include dynamics of the power electronic interface of a wind farm, with focus on the control structures while neglecting the dynamics of the switching operation. Eigenvalue analysis of the linearized system will be applied to evaluate the small signal stability of the system.

1.3 Outline of report

Chapter 2 is the main theory chapter serving as a model description, where the physics and mathematics of the simulation model is described. The model description has three main subchapters; the synchronous generator, wind power theory and inverter modeling. Chapter 3 gives an introduction to general stability theory with focus on explaining linear analysis and its applications in power system stability analysis. Chapter 4 presents simulation results from time domain simulations, linear analysis and sensitivity analysis. Then follows the chapters "Discussion", "Conclusion" and "Recommendation for further work". Chapter 8 is the appendix, including a brief discussion about liearization issues in Matlab, list of acronyms and abbreviations and the full simulation model.

2 Model description and theory

This chapter aims to give an explanation to the physical and mathematical background for the simulation model and to explain the assumptions made in the process. All parts of the model are built from scratch in Simulink/Matlab.

2.1 Dynamic modeling of synchronous generators

Dynamic simulations in power systems are time step simulations where the state variables of the system change and interact. Figure 1 shows a principal flowchart of a dynamic simulation for a 5th order model, meaning that each synchronous generator has five state variables. In the following subsections each of the steps in the simulation are explained[4].

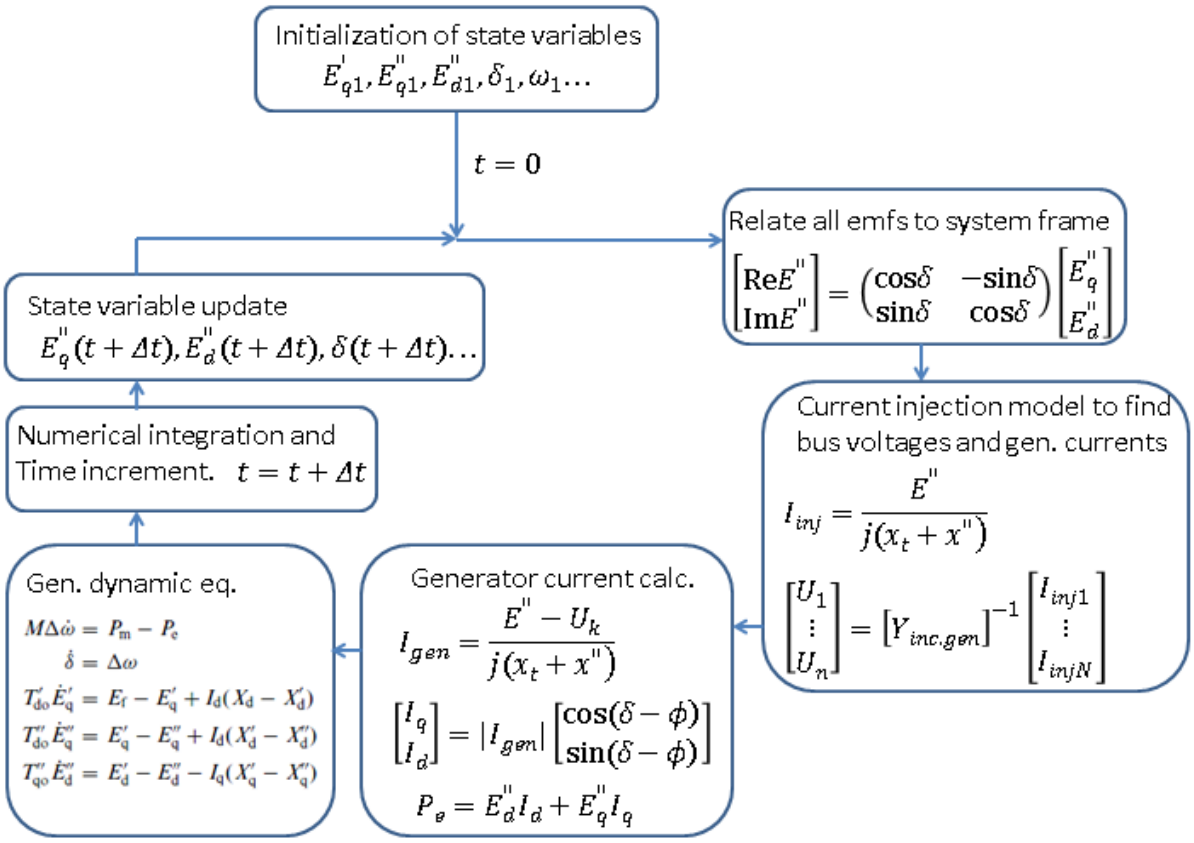

Figure 1: Flowchart of power system dynamic simulations.

2.1.1 Initialization

Briefly explained the state variables are the minimum set of variables necessary to describe a physical system. For the synchronous generator the state variables generally are internal emf, rotor speed and angular displacement from the reference machine. The principle assumes that once the state variables are known, all other parameters such as currents, powers, bus voltages, etc, can be calculated. Before the simulation starts, the initial values of the state variables must be known. These are found from load flow calculations and knowledge of the generators transient and subtransient reactances. If the initial condition is not the equilibrium point, there will a transient period to establish an "equilibrium" point, however the accuracy of the initialization may determine if a stable operating point is established.

2.1.2 The dq-reference frame

In order to simplify the difficult geometry of the 3-phase stator winding of a synchronous generator, a 2-axis reference system is introduced. The reference frame is based upon rotor position, where the magnetomotoric force from the field winding defines the direct axis or d-axis, while the quadrature axis or q-axis, lags 90°. In the synchronous generator the three phase sinusoidal stator winding, under balanced conditions in steady state, creates voltage and current space vectors of constant magnitude rotating at synchronous speed. Figure 2 shows the relation between the rotor position, the dq-axes and the space vector representation of emfs, voltages and currents. The figure illustrates how the space vector representation of terminal voltage and current are decomposed into components parallel to the d- and q-axis. The angle δ_g between the emf, $\underline{E}_f$, and the terminal voltage $\underline{V}_g$is called the power angle as the electric power is heavily dependent on this angle through equation 1.

$$P = \frac{E_q V_g}{X_d} sin\delta_g + \frac{V_g^2}{2} \frac{X_d - X_q}{X_d X_q} sin2\delta_g \tag{1}$$

However, it should be emphasized that the angle δ_g is not the same as the state variable δ. In dynamic simulations, the q-axis of one of the generators is utilized as a system reference frame, the state variable δ_n is the angular difference between the q-axis of generator n and the q-axis of the system reference frame.

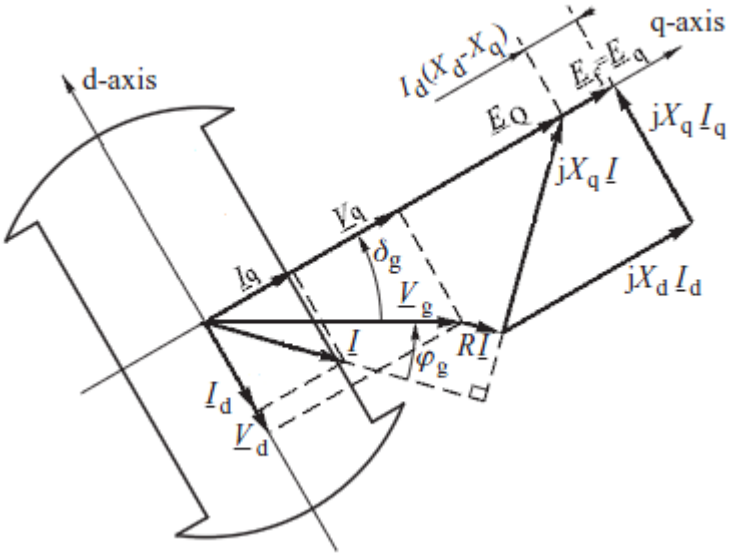

Figure 2: Salient rotor dq-axes and phasor diagram. Figure 3.16 in [2] modified.

2.1.3 Transient modeling

The model of a synchronous generator is an electromotive force, emf, behind a synchronous reactance. Dynamic simulations utilize the same approach, but include the impact of how dynamics in the generator current interact with the electromotive force through different magnetic flux screening effects. In this project a 5th-order model is utilized, this means each generator is represented by the five states; rotational speed deviation ($\Delta\omega$), relative rotor angular displacement refered to reference machine (δ) , q-axis transient emf $E_q^{'}$, q-axis subtransient emf $E_q^{''}$and d-axis subtransient emf $E_d^{''}$. There are five differential equations representing changes in the generator state variables.

$$2H\dot{\Delta\omega} \quad = \quad P_m - P_e \tag{2}$$

$$\dot{\delta} = \Delta\omega_{rel} \tag{3}$$

$$T_{do}^{'}\dot{E_q^{'}} = E_f - E_q^{'} + I_d(x_d - x_d^{'}) \tag{4}$$

$$T_{do}^{''}\dot{E}_{q}^{''} = E_{q}^{'} - E_{q}^{''} + I_d(x_d^{'} - x_d^{''}) \tag{5}$$

$$T_{qo}^{''}\dot{E}_{d}^{''} = E_{d}^{'} - E_{d}^{''} - I_q(x_q^{'} - x_q^{''}) \tag{6}$$

Equation 2 introduces the inertia time constant, H, and can be interpreted as newtons second law of motion. Equation 3 relates the relative angular displacement to the relative speed deviation. Normally these equations are presented in litterature [2] with only one variable for speed deviation, $\triangle\omega$. However, this approach is only valid for simulations where the grid is represented as "stiff", meaning that the grid speed never changes. In order to model several machines in a system without a "fixed" grid two different speed deviations are needed. The first, $\triangle\omega$, is the deviation from the speed reference. The other, $\Delta\omega_{rel}$, is the speed deviation from the reference machine.

Equations 4 to 6 introduce the open circuit time constants, $T_{do}^{'}$, $T_{do}^{''}$, $T_{qo}^{''}$, which describe how fast the related emf is able to change. The physical background for these constants are the time constant of a RL-circuit, and relate to how the flux is able to change in a winding. The subtransient time constants $T_{do}^{''}$ and $T_{qo}^{''}$ relates to how fast flux is able to penetrate through the screening damper windings and the rotor body (which screen the flux by inducing eddy currents). These time constants are very rapid and according to [2] often in the range of less than 200 milliseconds.

The transient time constant $T_{do}^{'}$relates to how fast the flux is able to change through the field winding and is calculated as $T_{do}^{'} = \frac{L_f}{R_f}$. Since the inductance of the field wining is very large, this time constant is much larger, often up to 10 seconds. Generator data for the largest generators in the world [3], the 840 MVA units utilized in the Three Gorges project in China, are specified to have the time constants; $T_{do}^{'} = 10.1/11.1s$, $T_{do}^{''} = 0.1/0.075s$ and $T_{qo}^{''} = 0.15/0.2$. The time constants are not equal as there are two different manufacturers.

The reason for choosing the fifth order model over the third order model is not that the dynamics of the emfs are significantly changed. The reason is that the additional differential equations include the important effect of damper windings. In the third order model the effect is modeled as a

torque proportional to the speed deviation, which is a more uncertain way of modeling the damping effect.

2.1.4 Governor and AVR modelling

There are two main controllers influencing the dynamic performance of the synchronous generator; the AVR, controlling the generator voltage, and the governor, controlling the turbine power. The AVR is modelled as a DC excitation system as shown left in figure 3, values for the time constants are found in [2]. It should be noted that the AVR model does not include the saturation function or PSS functionality. The block diagram of the hydro governor is shown right in figure 3. This model does not include the water starting time, but is considered to be of satisfying accuracy for the purpose of this model.

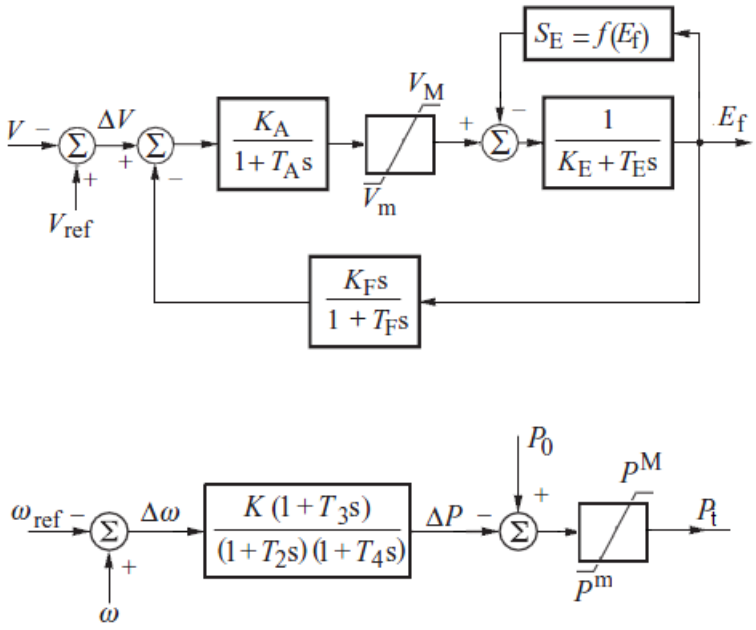

Figure 3: Block diagram of AVR (top) and governor equivalent (bottom). [2]

2.1.5 Overview of generator model

Figure 4 shows the Simulink implementation of a synchronous generator. In order to establish initial values for the emfs, the blocks $\frac{1}{T_x s+1}$ are replaced with a state space model with an appropriate initial condition. As all the currents and powers in the model are represented in per unit values, parameters such as inertia constants and the d- and q-axis reactances has to be referred to the system per unit bases. Figure 4 is an implementation of equation 2 to 6, describing the dynamics of the synchronous generator. It should be emphasized how the speed deviations are handeled.

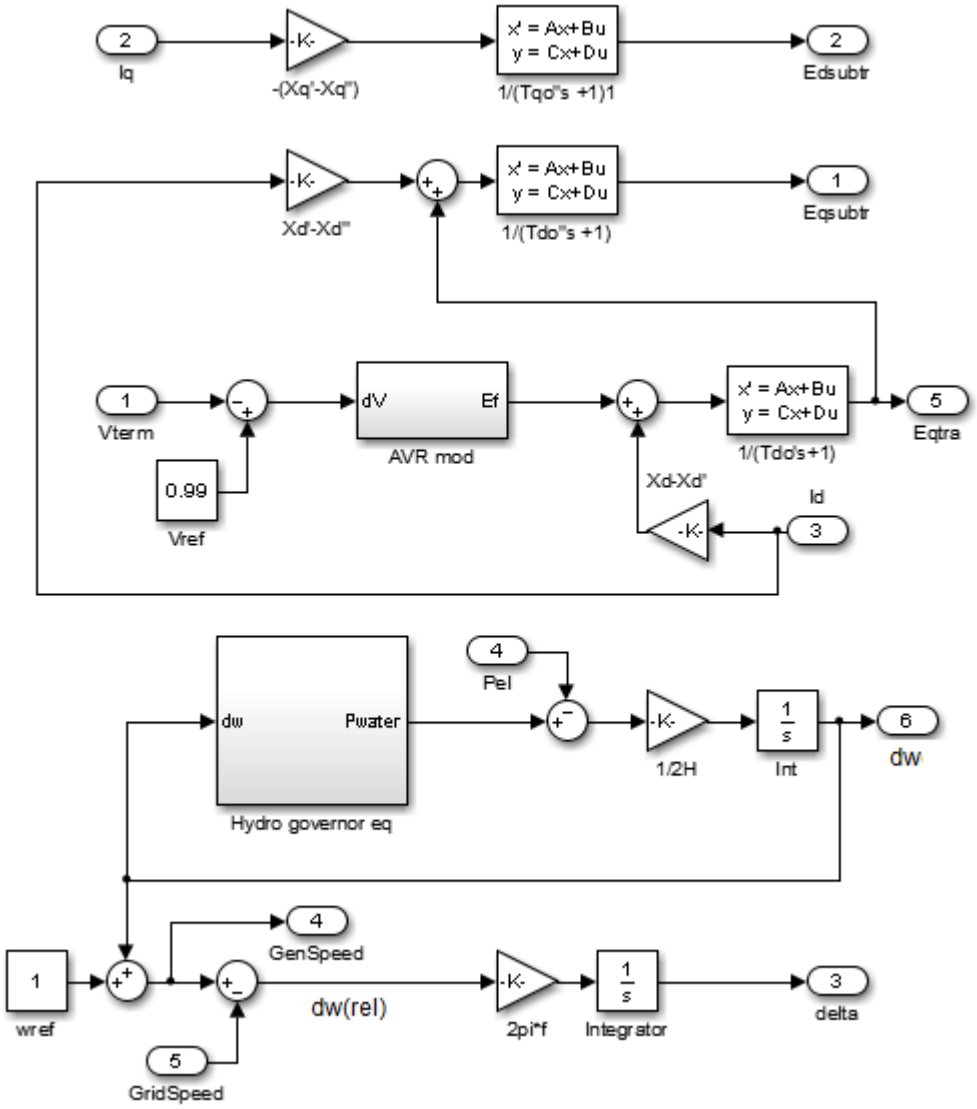

Figure 4: Synchronous generator model implemented in Simulink.

2.1.6 Algebraic equations

Purpose

The main part of the simulation model is built in accordance with the principle shown in figure 1. The implementation (without the wind turbine inverter

model) in simulink is a model consisting of two main parts. The first part is a subsystem as shown in figure 4 for each synchronous generator, here the five output ports represents the state variables of the generator. The second part is a large script that performs the algebraic equations the dynamic simulation flowchart. These equations are illustrated in figure 1 on page 3 labeled "Relate all emf to system frame", "Current injection model" and "Generator current calculation".

The aim of the script is to take the state variables of the generators as input and deliver the d- and q-axis currents, electric power and terminal voltage back to the dynamic equations to calculate the state variables of the next time step. Note that even though terminal voltage is not directly included in equations 2 to 6, it is the input signal to the AVR model, providing a value for the excitation emf, E_f.

Relation to the system reference frame

As the calculations are performed in the complex plane, it is desired to represent the emfs as vectors in the same coordinate system. The q-axis of a chosen generator is chosen as the real axis reference in the coordinate system, henceforth called the system reference frame. Figure 5 illustrates how the d- and q-axis subtransient emf through the angular displacement δ are related to the system reference frame. The transformation is implemented in the model as equation 7, relating all the emfs in the system to the same reference frame.

$$\begin{bmatrix} Re\left\{E''\right\} \\ Im\left\{E''\right\} \end{bmatrix} = \begin{bmatrix} cos\delta & -sin\delta \\ sin\delta & cos\delta \end{bmatrix} \begin{bmatrix} E''_q \\ E''_d \end{bmatrix} \tag{7}$$

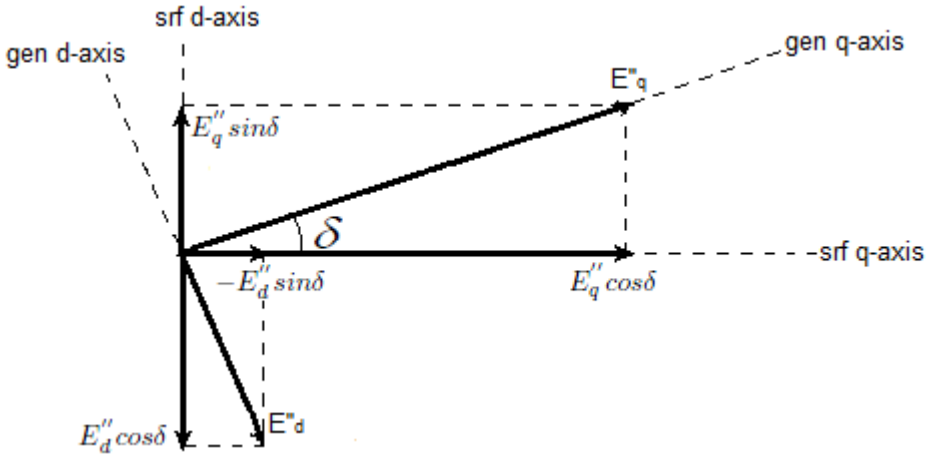

Figure 5: Relation from dq-axis emfs to a vector in the system reference frame.

Current injection model

The next step aims to find all the voltages in the system nodes. All the generators are modelled as subtransient emfs feeding their node through a subtransient reactance and transformer reactance in series. The idea is to create a Norton equivalent consisting of a current source directly feeding the node, but with a current division through a shunt reactance consisting of the subtransient reactance and the transformer reactance. The transformation is shown in figure 6. The injected current from generator K is given by equation 8, where $\underline{E}''$ is the vector representation of the subtransient emf in the system reference frame.

$$\underline{I}_{injK} = \frac{\underline{E}''_K}{j(x_{tK} + x''_K)} \tag{8}$$

Once the injected currents are known and arranged in a vector the system bus voltages can be calculated as equation 9. Here Y represents the admittance matrix of the current injection system, including the shunt branch consisting of transformer reactance and generator subtransient reactance from bus to ground.

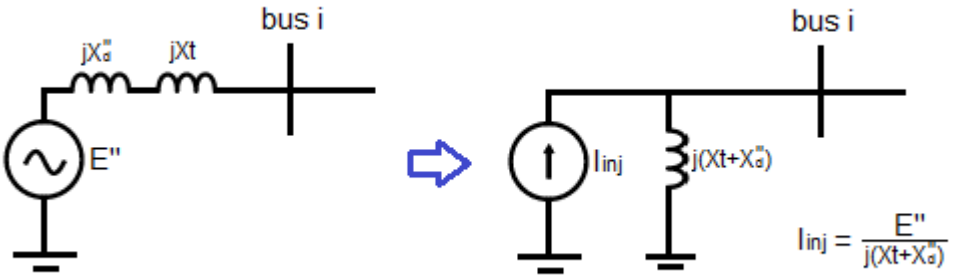

Figure 6: Circuit equivalents to the current injection model.

$$\begin{bmatrix} U_1 \\ \vdots \\ U_n \end{bmatrix} = \begin{bmatrix} Y \end{bmatrix}^{-1} \begin{bmatrix} I_{inj1} \\ \vdots \\ I_{injn} \end{bmatrix} \tag{9}$$

It should be noted that the load model in the basic model is a constant impedance load model.

Generator current calculation

This is the final step of the algebraic equations, the aim is to calculate the electric power and d- and q-axis current in each generator. The angular displacement δ is now utilized to trasform from the system reference frame back to the individual generator dq-frame. As both the bus voltages and the generator emfs are represented as vectors in the same reference system, the generator current in generator K is calculated as equation 10.

$$\underline{I}_{genK} = \frac{\underline{E}''_K - \underline{U}_K}{j(x''_K + x_{tK})} \tag{10}$$

Once the generator current is known, it can be decomposed into d- and q-axis components, as the angular displacement from the system, δ_K, is known. In the model values are scalar and not vector representations, however, as they are defined aligned to the generators d- and q-axis, they may be represented as vectors combined with δ_K. The d- and q-axis currents are calculated as equation 11, where φ_K is the angle of the generator current.

$$\begin{aligned} I_{qK} &= abs\left(\underline{I}_{genK}\right) \cdot cos(\delta_K - \varphi_K) \\ I_{dK} &= abs\left(\underline{I}_{genK}\right) \cdot sin(\delta_K - \varphi_K) \end{aligned} \tag{11}$$

When the d- and q-axis currents are known, the electrical power is calculated as equation 12. However, as the d- and q-axis subtransient reactances are assumed equal in this project, the last term disappears.

$$P_e = E_d^{''} I_d + E_q^{''} I_q + (x_d^{''} - x_q^{''}) I_d I_q \tag{12}$$

2.2 Wind power modeling and control

2.2.1 General theory

Due to the unpredictability of the wind the control strategy of wind power differs from traditional power production. The traditional control strategy is designed to maximize the energy capture. The mechanical power can be calculated by equation 13 where φ is air density, A is the area swept by the rotor blades and V is the wind speed. The coefficient of performance, c_p, is a function of pitch angle of the blades, β, and the tip speed ratio λ.

$$P_{mech} = {}^1\!/_2 \varphi A c_p(\lambda, \beta) V^3 \tag{13}$$

The power control is performed by controlling two parameters; the generator torque and the pitch angle of the blades.

2.2.2 Generator torque controller and inertia emulation

In all modern wind turbines there is a power electronic interface between the grid and the generator. Today the trend is leaning towards generator solutions with fully rated converters and synchronous generators, shown in figure 7.

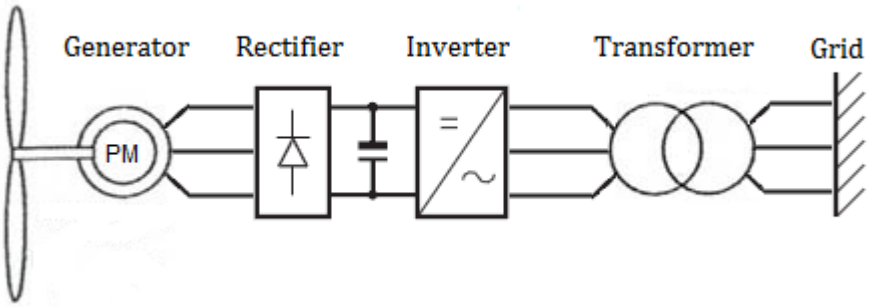

Figure 7: Grid interface of a permanent magnet synchronous generator .

The normal control strategy for the torque controller is to use the inverter to control the output torque. The normal approach is to use the the rotational speed of the turbine as input signal. This signal provides a reference torque for the inverter from a look-up table or a simple calculation. If the electric torque is larger than the mechanical torque the turbine will decelerate and the electric torque set point will decrease. The control and modelling of the inverter will be further explained in later chapters.

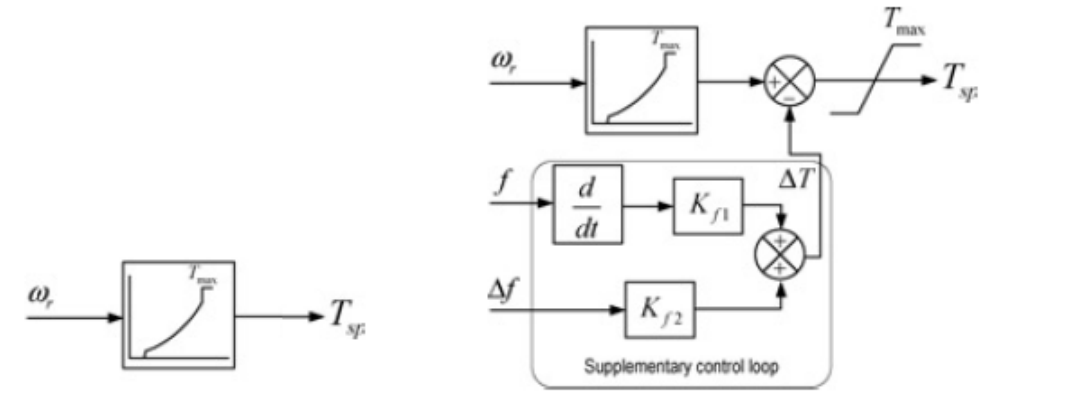

Figure 8: Torque controller without and with inertia emulation.[5]

Figure 8A illustrates the principle of a traditional torque controller. Figure 8B illustrates the working principle of a torque controller with inertia

emulation. With grid frequency as another input variable, the turbine can provide inertial response to changes in grid frequency. The additional torque is provided on two signals; frequency deviation and rate of change in frequency. Many simulations in literature [8][9] show that the synthetic inertia emulation is an important feature for the frequency stability in grids with significant amounts of wind power.

2.2.3 Pitch angle controller

The pitch angle control is performed by servo motors in the yaw, normally acting as a power limitation control. The pitch angle is optimal for wind speeds below rated wind speed. When the wind increases above rated wind speed the available power exceeds the power capture ability. The pitch angle is now used to reduce the coefficient of performance to limit the power capture. Figure 9 illustrates the impact on coefficient of performance from different pitch angles.

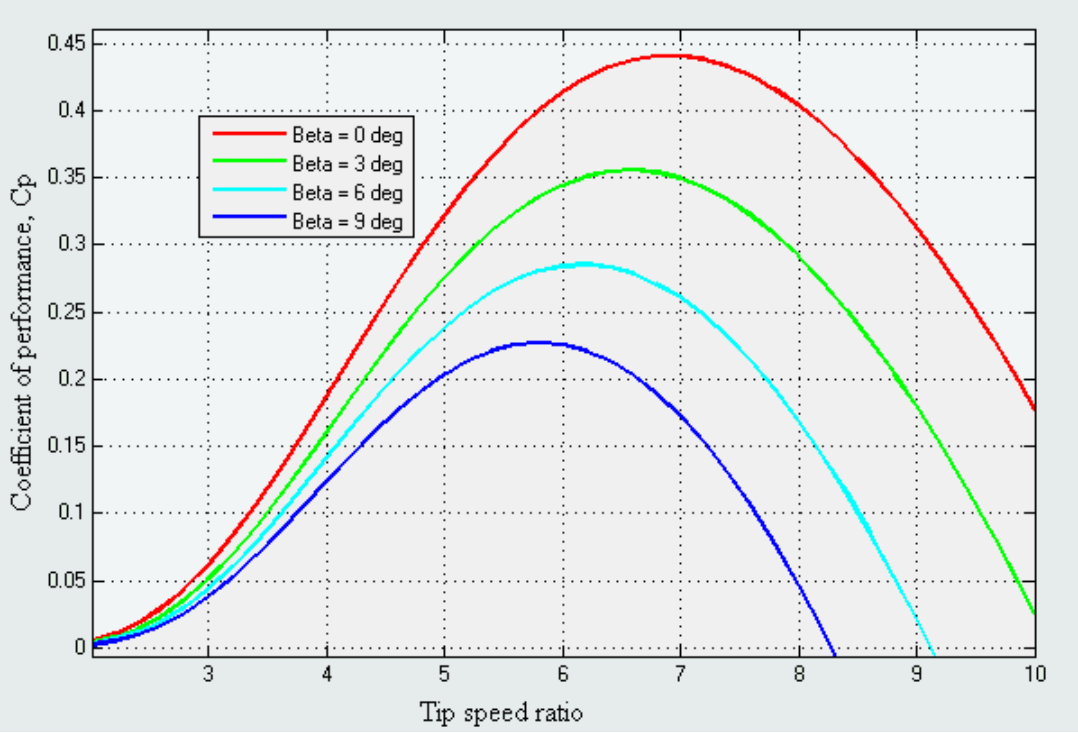

Figure 9: Pitch angle versus coefficient of performance.

2.2.4 Modelling of wind turbine

The specialization project report gives a detailed teoretical background forthe wind turbine model. The model utilized in the specialization project takes the wind speed, frequency deviation and a power reference as input signals and delivers electric power and estimated available power as output signals. The model used in this project is somewhat modified and takes wind speed, electric power and terminal frequency as input signals and delivers a torque set point (without the inertial torque) to the inverter model.

The difficult part of the wind turbine model is to calculate the mechanical torque and particularly the coefficient of performance. The approach is to calculate the coefficient of performance with a numerical approximation as in [2]:

$$C_p = 0.73\left[(151/\lambda_i) - 0.58\beta - 0.002\beta^{2.14} - 13.2\right] e^{(-18.4/\lambda_i)} \tag{14}$$

where

$$\frac{1}{\lambda_i} = \frac{1}{\lambda - 0.02\beta} - \frac{0.003}{\beta^3 + 1} \tag{15}$$

and β is the pitch angle of the blades. The entire wind turbine model is included in the appendix.

2.3 Inverter modeling and control

Illustrated in figure 7 on page 14 the electric interface between the turbine and the grid is the inverter. The purpose of the inverter is to feed a three phase AC-system from a DC source. The inverter is assumed to be fed from a constant DC source and controls the output current and voltage. The inverter utilizes semiconductor technology such as IGBTs or MOSFETs for switching, and through pulse-width modulation creates an approximation to the fundamental sine wave. The voltage source inverter is a very fast component and the ability to follow a power or voltage reference is limited with a time constant $T_s = 1/f_s$ where f_s is the switching frequency, often several kHz.

2.3.1 Inverter model

The model considered most suitable for electromechanical stability analysis in large power systems is the average model. The approach is to neglect the switching dynamics of the inverter and represent it as a three phase voltage source at the inverter terminals.

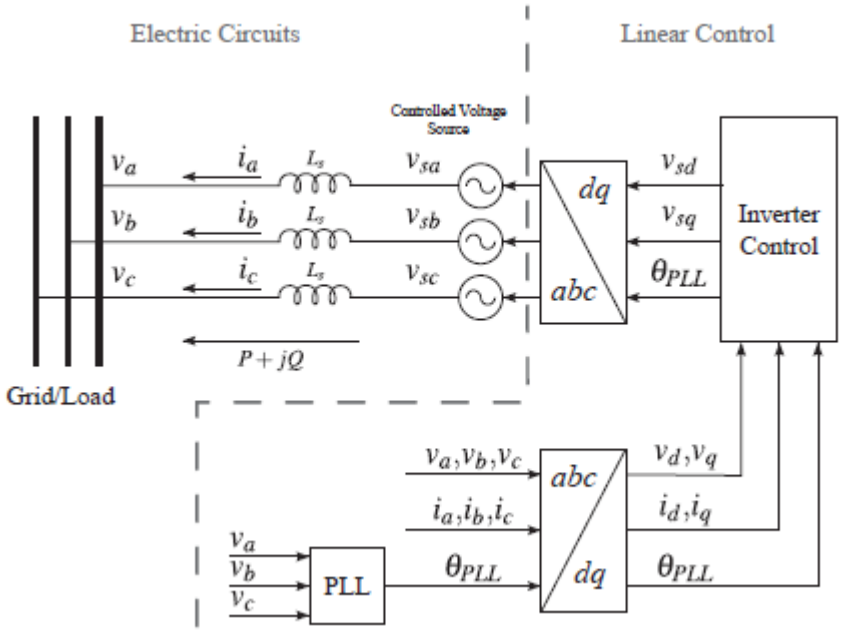

Figure 10: Principle of the average inverter model.[6]

Figure 10 illustrates the average model of the inverter. However, there are several differences between this model and the simulink model utilized. The average model in figure 10 includes phase voltages, and therefore needs the phase lock loop angle θ_{PLL} for the transformations between the abc and dq reference frames. This is the real way to control the inverter, however it is considered unnecessary difficult to implement in simulink, as the entire model operates in the dq-reference frame.

In the current injection model the inverter is modeled as an emf behind a transformer reactance, similar to the synchronous generators (without the subtransient synchronous reactance). However, the dynamics of this emf

differs from the synchronous generators. Considered as a "black box"-model the inputs of the inverter are the terminal voltage, voltage angle refered to the system reference frame q-axis, and d- and q-axis currents, also refered to in the system reference frame.

2.3.2 Power and current control

Inconveniently the reference frames used for synchronous generators and inverters are not the same. The synchronous frame aligns the q-axis to the excitation emf while the d-axis leads by 90 degrees. The dq-reference frame utilized in power electronics on the other hand, aligns the d-axis to phase A of the terminal voltage of the inverter while the q-axis leads by 90 degrees. The reason for this is that with the absence of q-axis voltage the dq-composed currents are translated to active and reactive current through:

$$\begin{aligned} P &= V_d I_d \\ Q &= -V_d I_q \end{aligned} \tag{16}$$

Hence controlling the d-axis current is the equivalent of controlling the power output. By controlling the q-axis current either terminal voltage or reactive power can be controlled. The only limitation of the reactive capability is the current rating of the inverter compared to the active current. Figure 11 illustrates the principal control structure in an inverter. As the current is decomposed the power deviation translates to a change in d-axis current, whereas the voltage deviation translates to a change in q-axis current to change the reactive power output. This principal structure does not include a current magnitude limitation nor the angular displacement from the system reference frame.

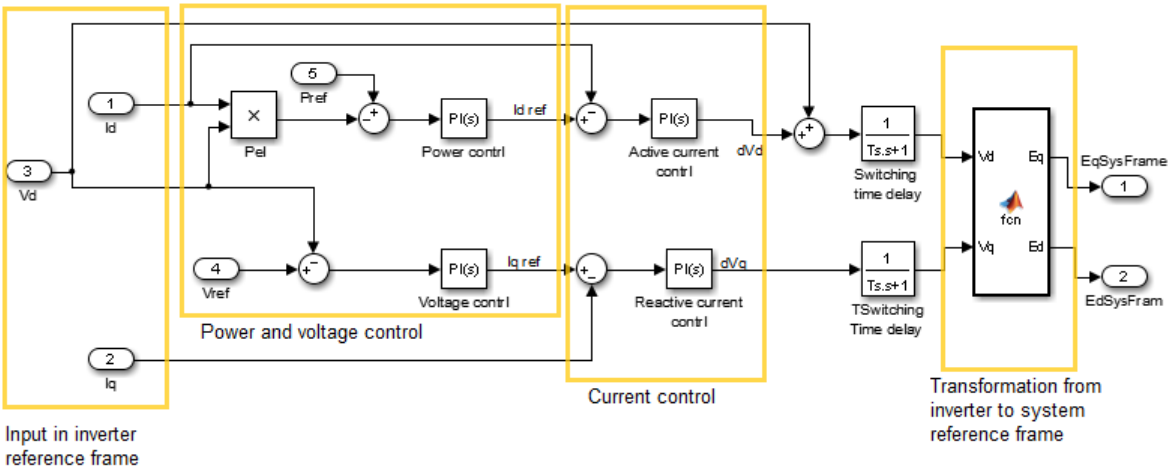

Figure 11: General control structure of the inverter.

2.3.3 Inertia emulation

As seen in figure 8 on page 14, the principle of inertia emulation is to take grid frequency as input signal and provide an additional electric torque to counteract changes in frequency. Here it is vital to emphasize that "grid frequency" is a relative term. At every bus in the grid the frequency is $f_n = f_{ref} + \frac{d\delta_n}{dt}$ where f_{ref} is frequency at the reference bus (speed of reference machine) and δ_n is the voltage angle at bus n. In a synchronous generator a change in voltage angle is closely related to change in power angle, which is the mechanism behind the inertial response in the synchronous generator. An issue arises as the inverter is able to change the power output so rapidly, that the $\frac{d\delta_n}{dt}$ term becomes significant.

As an illustration; a power plant of significant size loses its connection to the grid. The frequency in the entire grid will start to fall and synchronous generators will provide inertia. The wind farm inverter will detect the frequency fall and the derivative term will immediately create a rapid increase in the power reference. This additional power output may increase the voltage angle δ very rapidly, this again will lead to a frequency rise at the terminals due to the derivative term in $f_n = f_{ref} + \frac{d\delta_n}{dt}$. This leads to difficulties in the model due to the rapidness of the switching time constant. However, these are only mathematical problems. The frequency measurement will be

sampled at a certain rate and act as a low pass filter. When "experimenting" with inertia emulation in the model the time constant of this filter, the PI controllers in the inverter and the proportional and derivative gains of the inertia loop is adjusted. Figure 12 illustrates the implementation of the inertia emulation. The terminal frequency is calculated in p.u. as the sum of the speed of the reference machine and the time derivative of the voltage angle at the bus.

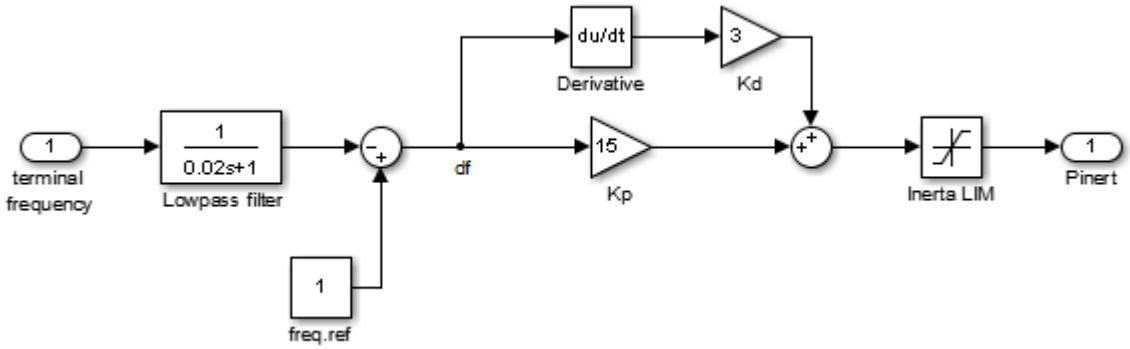

Figure 12: Simulink implementation of synthetic inertia.

2.3.4 Inverter model overview

Figure 13 shows the actual Simulink implementation of the inverter and turbine. The mathematical trick here is that the voltage angle relative to the system reference is assumed known.

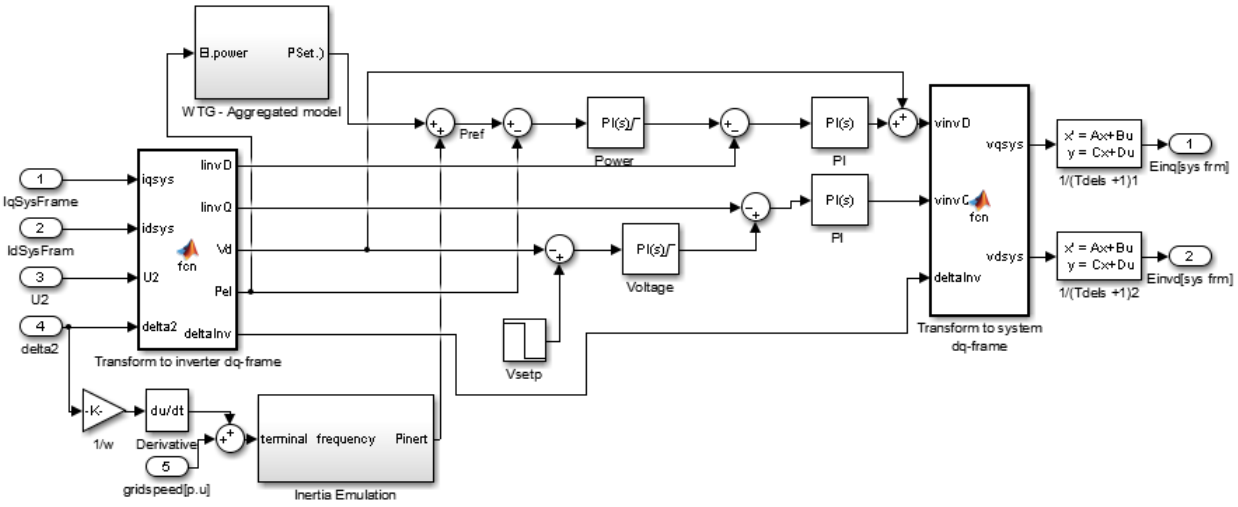

Figure 13: Full implementation of inverter model in Simulink.

3 General theory of power system stability

3.1 Definitions of stability

Power system stability is normally categorized into three different classifications; voltage stability, frequency stability and rotor angle stability[2]. Voltage stability is related to load dynamics and the ability to provide and consume reactive power. Voltage stability is not studied in this project. Frequency stability is related to the power balance in the system and the dynamics of the frequency response of the system, these issues were discussed in the specialization project. Rotor angle stability relates to the electromechanical phenomenons of synchronous generators and their capability to remain stable after a physical disturbance.

This project will focus on the impact on rotor angle stability from synthetic inertia from wind farms. Rotor angle stability is often divided into small signal stability and transient stability. This is due to the nonlinearities in the physical system, where small signal stability analysis often utilizes a linearized system and is only valid for small disturbances around the linearized operating point.

To understand the dynamic behavior of the power system a matematical model based on the physical laws and structures in the system needs to be built. As the system is extremely large and complex a model is a compromise between complexity and accuracy. Most dynamic models for rotor angle stability are based on a state space representation. The system state variables are the variables necessary to define the operating condition. Once the state variables are known, all other parameters in the system can be calculated. The entire system can be represented by the state vector

$$\mathbf{x}=\begin{bmatrix} x_1 \\ \vdots \\ x_n \end{bmatrix} \tag{17}$$

where $x_1, \cdots, x_n$ are the state variables of the system. These state variables can represent values such as voltages, rotor speeds and angular deviations. A normalized state vector will define an operating point in the n-dimensional state space, this operating point in the state space is often referred to as the "system state".Figure 14 illustrates the Lyapunov definition

of stability of a system[2]. The equilibrium point in the state space is $\hat{x}$, while x_0 is the operating point at $t = 0$. If, during $t \to \infty$, the system state reaches the equilibrium point (and stays there) the system is said to be asymptotically stable. If the system state does not reach the equilibrium point, but never is further away from it than a finite distance ε, the system is said to be stable. If the system state leaves the ε-limit, the system is said to be unstable.

The Lyapunov definition of stability is that the system is stable if there exists a distance η in the state space, larger than zero, so that all system states closer to the equilibrium point than the distance η is stable.

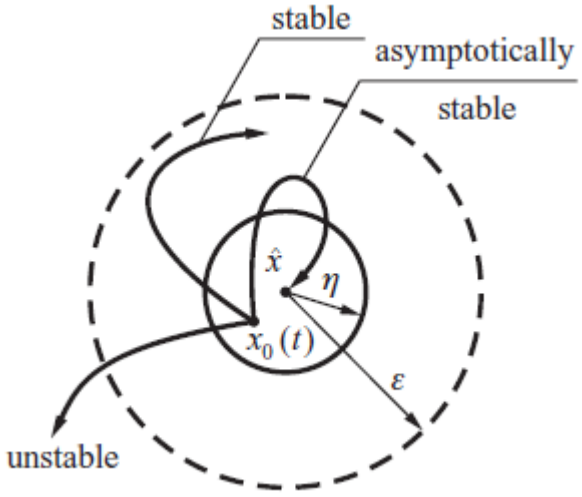

Figure 14: Illustration of Lyapunov stability criteria used by [2].

3.2 Linear analysis

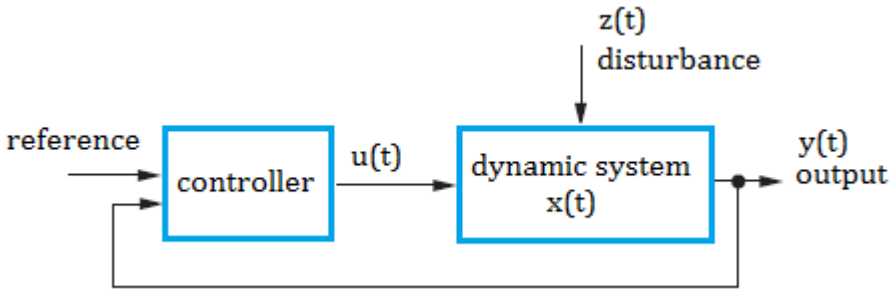

Figure 15: Structure of a closed loop controlled system. .

Linear analysis is a tool often utilized in systems represented by a state space model. The system state, $\mathbf{x}$, is a column vector containing the n state variables of the system; x_1, x_2, $\ldots x_n$. In dynamic simulations the state variables interact and change with time, so that

$$\mathbf{x}(t) = \begin{bmatrix} x_1(t) \\ x_2(t) \\ \vdots \\ x_n(t) \end{bmatrix}. \tag{18}$$

In the model described in chapter 2.1, the matematical state variables may be difficult to identify as the model is created to illustrate the dynamic behavior in time. It may be even more difficult to identify the equations describing the interaction between the state variables. However, it is possible to describe the system as a neat system of ordinary differential equations. Equation 2 to 6 illustrates how these differential equations are outlined. Here ω, δ, E_q', E_q'', E_d'' are the state variables. These equations illustrate the principle of the structure of the system of ordinary differential equations which generally are written as

$$\dot{\mathbf{x}} = \mathbf{F}(\mathbf{x}, \mathbf{u}) \qquad \mathbf{y} = \mathbf{G}(\mathbf{x}, \mathbf{u}) \tag{19}$$

where u and y represent the control signals and output signals of the system, referred to figure 15. $\mathbf{F}(\mathbf{x}, \mathbf{u})$ is a column vector of equations describing the differential equations, which may be both nonlinear or linear equations.

$\mathbf{G}(\mathbf{x}, \mathbf{u})$ represents the equation set to calculate the chosen output variables. If the system only contains linear equations, the system is linear and can be described by

$$\dot{\mathbf{x}} = \mathbf{A}\mathbf{x} + \mathbf{B}\mathbf{u} \qquad \mathbf{y} = \mathbf{C}\mathbf{x} + \mathbf{D}\mathbf{u} \tag{20}$$

Where $\mathbf{A}, \mathbf{B}, \mathbf{C}, \mathbf{D}$ are matrixes.

Generally the differential equations in a dynamic power system model contain nonlinear equations. These unlinearities are due to phenomenons such as the sine dependency between electric power and angular displacement seen in equation 1, limitations and other nonlinear phenomenons. However, through a linearization process, one can obtain a linearized system which contains important information of the system stability. The linearized system is only valid for small deviations around the operating point where the difference between the linearized model and the nonlinear model is minimal. Hence to utilize linear analysis to evaluate system stability is also called to evaluate the "small signal stability" of the system. The process is to transform the representation in equation 19 to a linear model as in equation 20. To to this the equation sets are derivativated with respect to $\mathbf{x}$ and $\mathbf{u}$, such that

$$\begin{aligned} \mathbf{A} &= \tfrac{dF}{dx} \\ \mathbf{B} &= \tfrac{dF}{du} \\ \mathbf{C} &= \tfrac{dG}{dx} \\ \mathbf{D} &= \tfrac{dG}{du} \end{aligned} \tag{21}$$

and the linear approximation becomes

$$\triangle\dot{\mathbf{x}} = \mathbf{A}\triangle\mathbf{x} + \mathbf{B}\triangle\mathbf{u} \qquad \triangle\mathbf{y} = \mathbf{C}\triangle\mathbf{x} + \mathbf{D}\triangle\mathbf{u} \tag{22}$$

There exists a linear analysis tool in Simulink that performs this transformation and returns, the linearized system as a state space model.

So the system can be represented as a linear approximation, and one may ask; what is interesting about this? From a stability point of view this is very interesting due to the fact that once the linear system is known, the system response can be predicted using eigenvalue or modal analysis. The linear

system contains information about the oscillatory behavior; which frequencies will the response contain, how well is the damping of these frequencies, which state variables will be subjects to the different frequencies. This is important information about the system stability and is the reason for utilizing eigenvalue analysis.

3.3 Eigenvalue analysis

3.3.1 Eigenvectors

In a system of linear differential equations described by the square matrix $\mathbf{A}$, where

$$\dot{\mathbf{x}} = \mathbf{A}\mathbf{x} \tag{23}$$

there exists a trivial solution, given by $x(t) \equiv 0$. However, it is also expected that the equation system has a non-trivial solution on the form

$$\mathbf{x}(t) = \mathbf{W}e^{\lambda t}, \qquad \mathbf{W} = [\mathbf{w_1}, \ldots, \mathbf{w_n}] \tag{24}$$

where $\mathbf{w}$ is a non-zero constant vector and λ a scalar. Here $\mathbf{w_1}$, ..., $\mathbf{w_n}$ is said to be the eigenvectors of the system. While λ is called an eigenvalue. The following example illustrates the informations contained in eigenvectors. Assuming a system has 2 differential equations, two eigenvalues and two eigenvectors. Here the non-trivial solution will look like

$$\mathbf{x}(t) = c_1 x_1(t) + c_2 x_2(t) = c_1 \mathbf{w_1} e^{\lambda_1 t} + c_2 \mathbf{w_2} e^{\lambda_2 t} \tag{25}$$

If the two eigenvalues and the eigenvectors are $(\lambda_1, \lambda_2) = (3, 7)$, and $\mathbf{w_1} = \begin{bmatrix} 0.5 \\ -4 \end{bmatrix}$,$\mathbf{w_2} = \begin{bmatrix} 2 \\ -1 \end{bmatrix}$. Then the non-trivial solution is

$$\mathbf{x}(t) = c_1 \begin{bmatrix} 0.5 \\ -4 \end{bmatrix} e^{3t} + c_2 \begin{bmatrix} 2 \\ -1 \end{bmatrix} e^{7t} \tag{26}$$

or written as state variables

$$\begin{aligned} x_1 &= 0.5c_1 e^{3t} + 2c_2 e^{7t} \\ x_2 &= -4c_1 e^{3t} + -1c_2 e^{7t} \end{aligned} \tag{27}$$

Here c_x is the initial condition. The eigenvectors provide information about how the different state variables are affected be each eigenvalue. In

power system stability analysis, the most interesting eigenvalues and elements in the eigenvector matrix are complex values. Complex eigenvalues give an oscillatory response (discussed below), and the complex elements in the corresponding eigenvector will tell us the magnitude and phase of the oscillation related to the eigenvalue.

The eigenvectors are found in the matrix $\mathbf{W}$, where each column is an eigenvector. To find the eigenvector element of state i to the corresponding eigenvalue j the element w_{ij} is found, as illustrated:

$$\mathbf{W} = \begin{bmatrix} w_{11} & \cdots & w_{j1} & \cdots & w_{m1} \\ \vdots & \ddots & \vdots & \iddots & \vdots \\ w_{1i} & \cdots & w_{ij} & \cdots & w_{mi} \\ \vdots & \iddots & \vdots & \ddots & \vdots \\ w_{1m} & \cdots & w_{jm} & \cdots & w_{mn} \end{bmatrix} \tag{28}$$

The element w_{ij} tells us how state variable i will be subject to the jth eigenvalue through (assuming non-complex eigenvalues):

$$x_i(t) = \ldots + c_j w_{ij} e^{\lambda_j t} + \ldots \tag{29}$$

Before the eigenvectors are utilized to create mode shapes, the properties of the eigenvalues will be discussed.

3.3.2 Eigenvalues and modes

Consider equation 23 on the previous page. The trivial solution is known as $\mathbf{x}$ being identical to zero. However, the non-trivial solution will exist if, and only if

$$det(\mathbf{A} - \lambda \mathbf{I}) = 0 \tag{30}$$

where $\mathbf{I}$ is the identity matrix. This equation determines the eigenvalues, λ, of the system. The eigenvalues can be real numbers, or appear as complex conjugate pairs. The eigenvalues are the base of the modes of the system. A real eigenvalue corresponds to a mode, while a complex pair of eigenvalues correspond to an oscillatory mode. To illustrate this, assume a system with three eigenvalues.

$$\begin{aligned} \lambda_{1,2} &= \alpha \pm \omega \\ \lambda_3 &= \beta \end{aligned} \tag{31}$$

Here $\lambda_{1,2}$ will create an oscillatory mode with a general behavior $e^{\alpha t}cos(\omega t)$, while λ_3 will create a mode with the behavior $e^{\beta t}$. From the exponential term it is obvious that for a linear system to be asymptotically stable the real part of all eigenvalues needs to be negative to provide a response where $\triangle \mathbf{x}$ tends towards zero, not infinity. While the frequency of the eigenvalue is directly given by the imaginary part, another important property is the damping. The relative damping is calculated as $\xi = \frac{-\alpha}{\sqrt{\alpha^2+\omega^2}}$ and provide information about how fast the mode approaches zero.

It can be shown[2] that the response of the state variables can be expressed

$$\mathbf{x}(t) = \mathbf{W}e^{\Lambda t}\mathbf{z_0} \tag{32}$$

Where $\mathbf{W}$ is the matrix of eigenvectors, $\mathbf{z_0}$is the initial condition of the modal variables and $e^{\Lambda t}$ is diagonal matrix of eigenvalues

$$e^{\Lambda t} = \begin{bmatrix} e^{\lambda_1 t} & 0 & 0 \\ 0 & \ddots & 0 \\ 0 & 0 & e^{\lambda_n t} \end{bmatrix} \tag{33}$$

The link between the initial state variables, $\mathbf{x_0}$, and the initial modal variables are $\mathbf{z_0} = \mathbf{W^{-1}x_0}$. Also, the modal variables can be expressed as $\mathbf{z}(t) = e^{\Lambda t}\mathbf{z_0}$. Therefore the response in the state variables can be expressed

$$\mathbf{x}(t) = \mathbf{W}\mathbf{z}(t) \tag{34}$$

As the initial state variables is a vector, not a matrix, the modal variables are found in a vector. Now relating back to equation 29, the response in the state variable i from the jth eigenvalue can now be expressed

$$x_i(t) = \ldots + w_{i,j-1}z_{j-1} + w_{i,j}z_j + w_{i,j+1}z_{j+1} + \ldots \tag{35}$$

In power system analysis the most interesting information is obtained from the eigenvector matrix, $\mathbf{W}$, and the eigenvalues, λ. The oscillations seen during dynamic events have a typical frequency of 0.2-2Hz. This corresponds to complex eigenvalues with an imaginary part of 1.2-12.5 rad/s. Identifying these eigenvalues and then identifying the corresponding elements in the eigenvector matrix provides information about which states the oscillation will occur.

Typically the states corresponding to generator speed are identified. If there are poorly damped eigenvalues the eigenvector elements will provide information of which generators beeing excited by the oscillation and how the phase shifts will be. This means that knowledge of the eigenvector matrix and the eigenvalues is sufficient to predict the small signal oscillatory response. To illustrate this see the following two examples.

3.3.3 Creating and interpreting mode shapes

The following plots and eigenvalues are extracted from the simulation model of a two area system, the operating point is not the same as in later chapters. There are three synchronous generators and one wind farm/inverter in the model. A further description will be given in later chapters. For a stable operating point the Simulink linear analysis tool is utilized to find the eigenvalues of the system. They are presented as a pole/zero map, where the poles represent the eigenvalues of the system. The reason for this representation is that Simulink requires variables for input and output to perform the linearization. The result of the linearization process is the system transfer function at the operating point. Hence, only the poles of the transfer function correspond to the eigenvalues.

From the eigenvalues a very poorly damped eigenvalue is identified at $-0.12 \pm j5.13$. This corresponds to an oscillation of $0.8Hz$ with a damping of only 2.4%. The linearized system is exported to Matlab as a state space model. Here the eigenvector matrix, $\mathbf{W}$, and eigenvalue diagonal matrix, e^{Λ} are calculated. Identifying the index of the eigenvalue and the index of the desired state variable, the desired elements can be extracted from the eigenvector matrix to create a mode shape plot. However, some issues should be noticed regarding the power system-idea of a state variable and Matlabs interpretation of a state variable. More about this topic is outlined in chapter 8.1 on page 57.

Example 1: Excitation emf

Figure 16 and 17 illustrate the application of mode shapes to predict the response. The mode shapes of the linearized system illustrate two key points. First, the magnitude of the oscillation will be more extensive in G3 and than

in G1. Second, the response will have very small phase shifts to each other. The time domain plot shows that this is valid, as the 0.8Hz oscillation seen in the excitation emfs are in phase, and is most visible in the predicted generator.

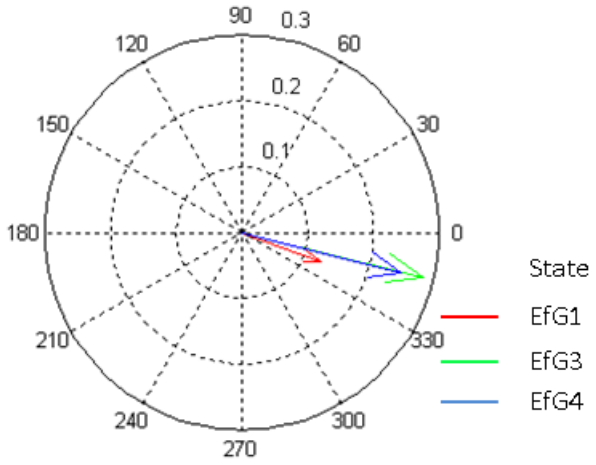

Figure 16: Mode shapes of excitation emfs to the poorly damped 0.8Hz mode.

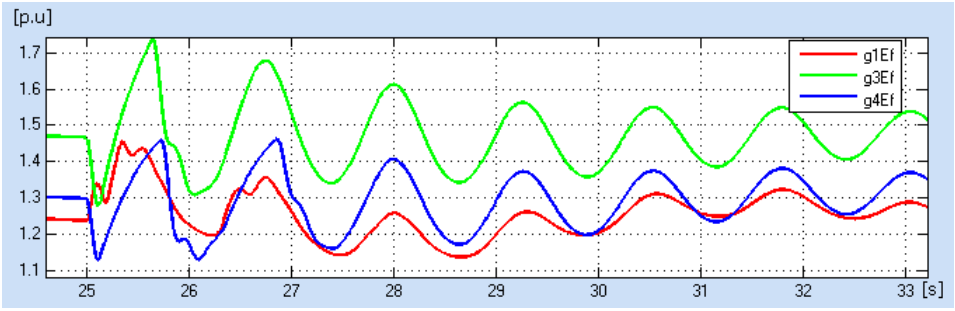

Figure 17: Time domain response in Ef.

Example 2: Speed deviation

The speed deviation is an important state variable as it is closely related to the angular displacement between the different generators. The angular displacement again generally determines the power transfer between the generators or areas, hence oscillatory behavior in the speed deviation translates

to oscillations in power transfer. Figure 18 and 19 illustrates the response in generator speed deviation. Notice that the oscillation now has a phase shift of nearly 180 degrees, visible both in the mode shapes and the time domain response.

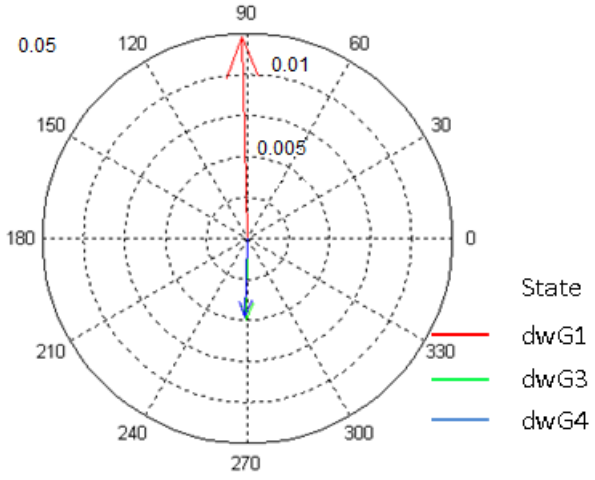

Figure 18: Mode shapes of generator speed deviation to the poorly damped 0.8Hz mode.

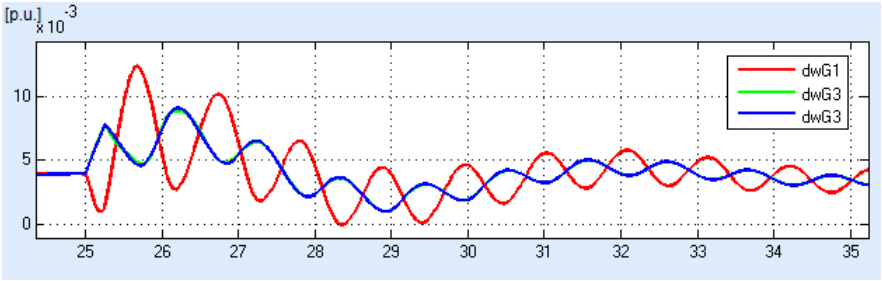

Figure 19: Time domain response in generator speed deviations (deviation from speed ref).

4 Simulations

The aim of the following section is to illustrate how synthetic inertia affects the stability of the system. Several studies have simulated how the frequency stability is "saved" by synthetic inertia as the share of wind power in the system rises [8][9]. These studies show that the inertial response from wind farms differ from the traditional synchronous generator response. Figure 20 is a simulation result illustrating the principal impact from synthetic inertia on frequency stability. The plots are all from a system with 40% wind penetration, the red graphs are the response with no inertial response, while the blue and green graphs are with synthetic inertia, but different controller tuning. Generally, results from such simulations are that with an increasing amount of inertia delivered the maximal frequency deviation decreases, while the time before recovery to acceptable frequency increases.

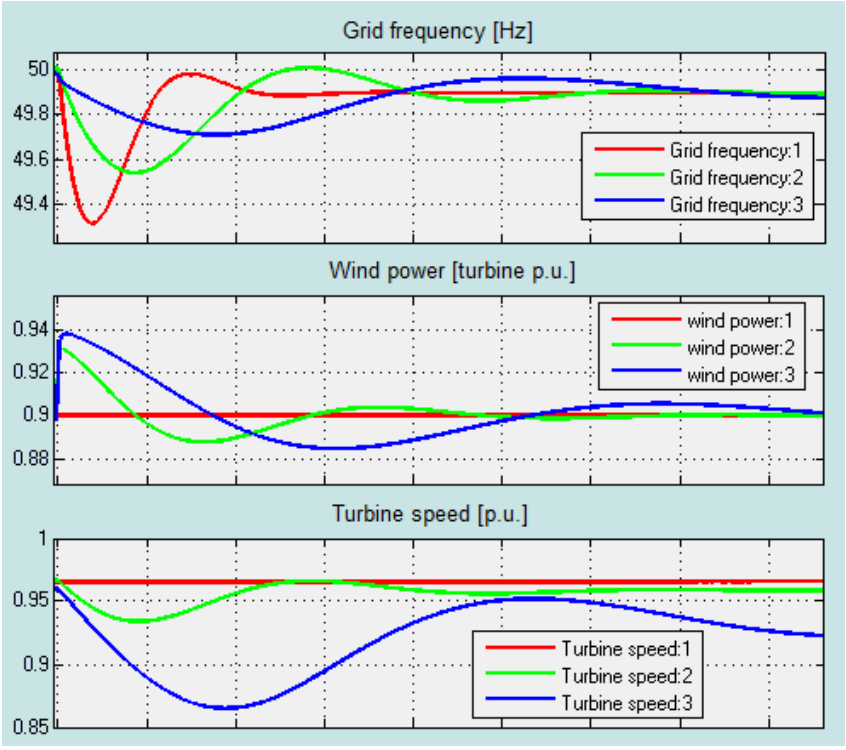

Figure 20: Typical simulation results from governor-based model. Figure from specialization project.

A drawback in these simulations, seen from a power system stability point of view, is that these models are "governor based". These simulations utilize the swing equation to model the grid frequency, while the dynamics of electric power is modelled as a sum of different governor responses. Here, all information about rotor angle stability is lost, and thus the inspiration of this master thesis; how the rotor angle stability is affected by synthetic inertia.

4.1 The two area system

Figure 21 illustrates the topology of the two-area system that has been implemented in Matlab/Simulink. The figure includes voltages and generation at the "base case" operating point. Notice that the apparent power in the figure is referred to as the bus injection. Also, notice that none of the voltage angles are used as reference, this is because the angular reference in the system is the q-axis of G3. It is assumed to be a hydro-based system with droop settings of 6% for all units.

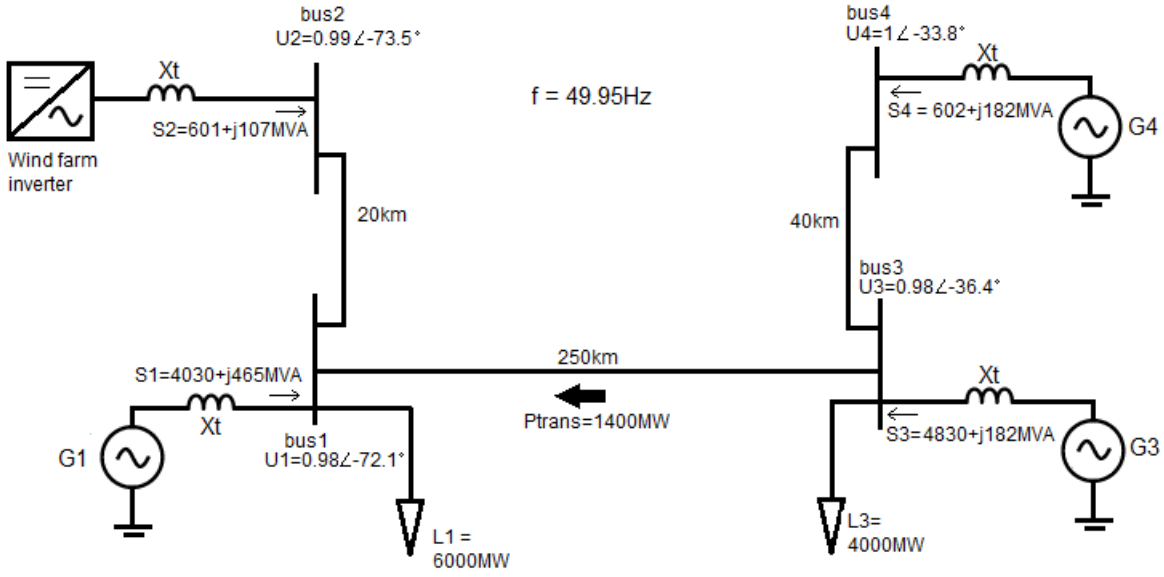

Figure 21: Topology of the 4-bus two area system.

The first simulations indicates the stability of the system without synthetic inertia. Here, some time plots and eigenvalue plots will be presented.

The next step will be to illustrate the effect of synthetic inertia. Some time plots will be presented, but mostly the eigenvalues of the linearized system will be studied. The idea is to illustrate how the eigenvalues move in the complex plane with different controller tuning for the inertia. Hopefully, this will result in a "suggested" controller tuning, that provides a significant inertial response and possibly improves the damping of the electromechanical eigenvalues. How synthetic inertia affects the critical clearing time of a fault will also be studied in this section. Finally the response with the suggested tuning will be compared to the response without synthetic inertia.

4.2 Stability of the system - without synthetic inertia

This section will present time plot responses to two different events, first a load connection event, then a fault at bus 3 will be simulated. Figure 22 presents the response in frequency and power outputs to a load connection of 600 MW. The response in power output from the inverter and G4 is presented in two different time scales. The right figure shows that after an inertial response in G4, the governor increases the turbine power corresponding to the droop setting. The left figure however, shows that the inverter power output is not constant. This is because the load increase causes disturbances in the grid voltages. This results in a change in the reference q-axis current in the inverter, which again causes a short dynamic response where power output is changed. This oscillation will later be named the "inverter mode".

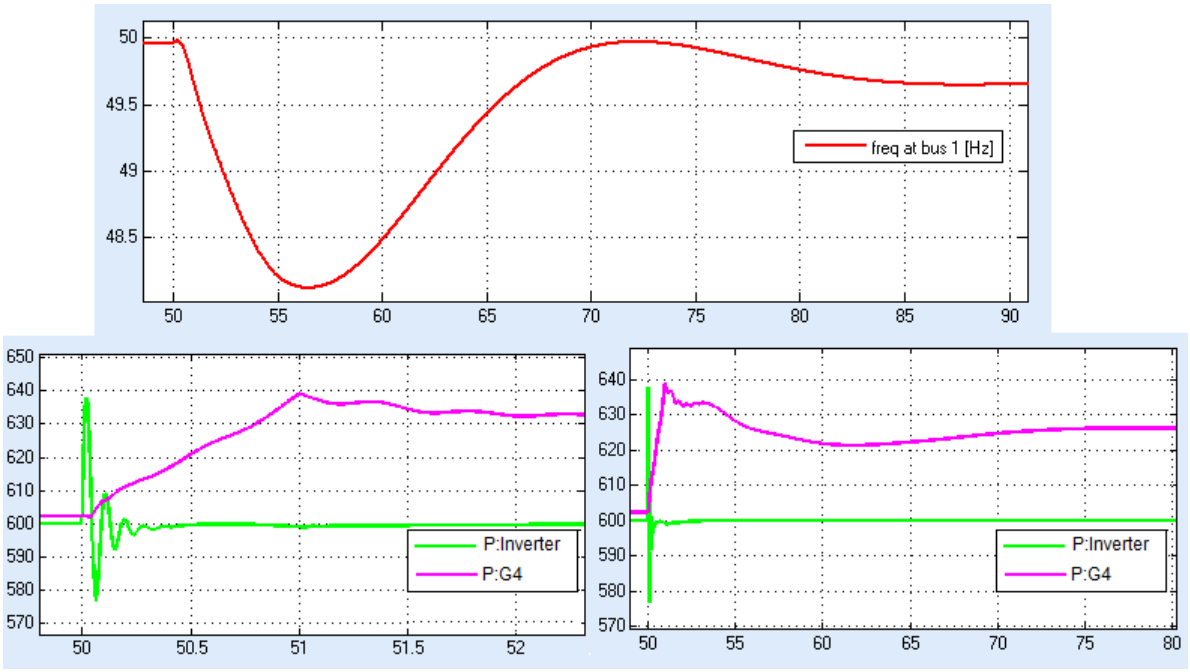

Figure 22: Frequency response and response in G4 and inverter to load increase event.

Figure 23 illustrates the time repose after a simulated fault. The fault is implemented as shunt resistance of 0.02 p.u for $80ms$ at $t = 50s$. The inverter at bus 2 behaves different than the synchronous generators, with a well damped high frequency oscillation immediately after the fault. The fault occurs at bus 3, this causes the voltage at bus 3 and 4 to drop much lower that on bus 1 and 2, therefore the acceleration is much faster at bus 3 and 4 as the generators ability to provide electrical torque is reduced. After $80ms$ the fault is cleared and electromechanical oscillations are visible. The most visible modes are two modes, one at $0.88Hz$ and the other at $2.34Hz$. These modes can be seen in the eigenvalues of the linearized system, shown in figure 24. It should be noticed that this is a pole-zero plot from Matlab. In this type of plot, only the poles, marked by crosses are the eigenvalues. This is because the pole-zero plot shows the poles and zeroes of the system transfer function, where only the poles correspond to the eigenvalues.

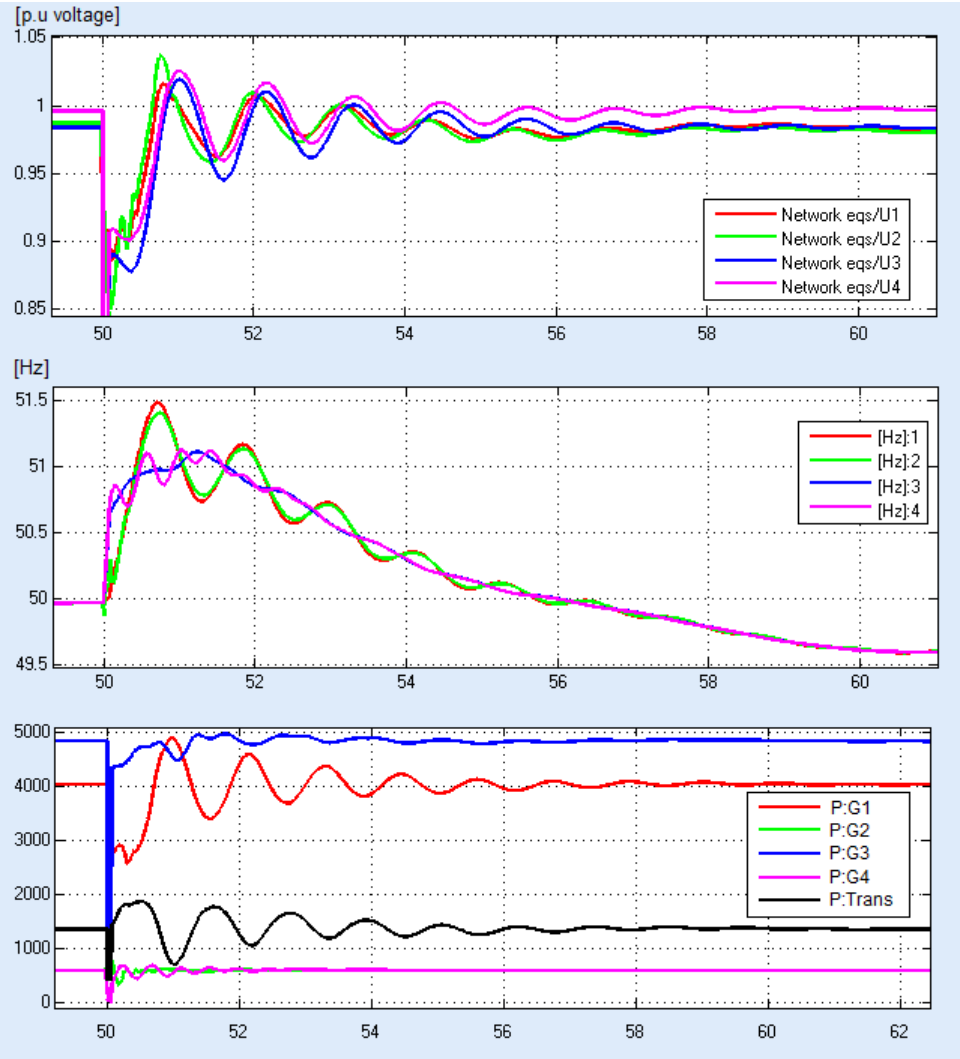

Figure 23: Response in voltages, bus frequencies and powers after fault.

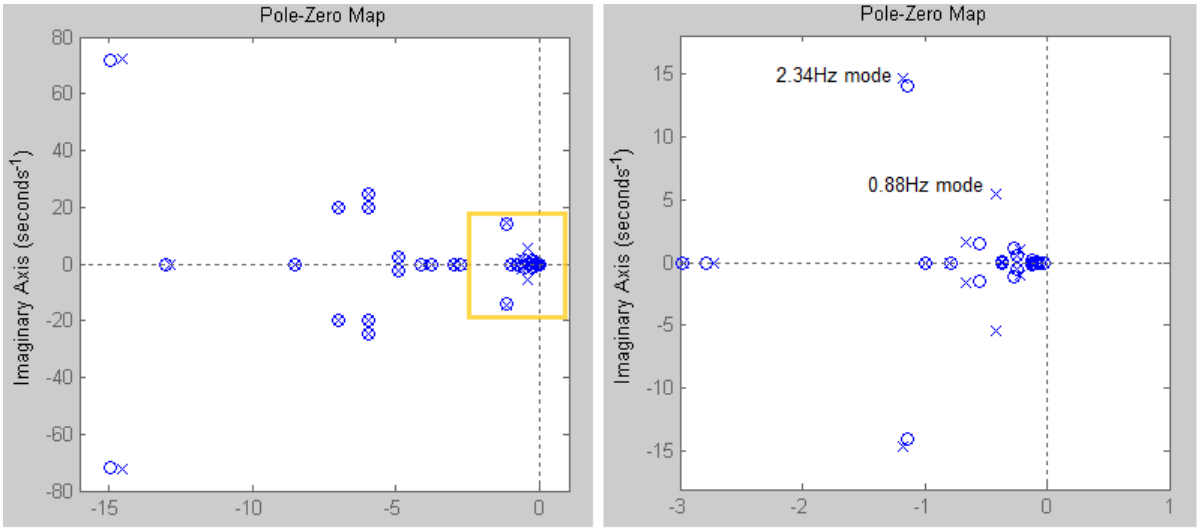

Figure 24: Eigenvalues of linearized system. Left; all eigenvalues. Right; zoomed to find the electromechanical eigenvalues.

The two most poorly damped modes (less than 10%) of the linearized system are listed in table 1. These eigenvalues will be compared to the eigenvalues when synthetic inertia is included in the model.

Eigenvalue no.	Value	Damping	Frequency
10,11	$-0.42 \pm 5.48i$	7.59%	$0.875Hz$
14,15	$-1.18 \pm 14.6i$	8.03%	$2.34Hz$

Table 1: Poorly damped electromechanical eigenvalues.

4.3 Synthetic inertia is implemented.

This section illustrates how synthetic inertia and inverter tuning affects the stability of the system. First, the impacts on eigenvalues as the inertia controller is more and more aggressive is illustrated. Second, the impacts on the eigenvalues from other parameters in the inverter controller are investigated. Finally, the differences between transient stability and small-signal stability will be illustrated by studying how the different control parameters affect the critical clearing time of a fault.

4.3.1 Increasing inertia controller gains

For the system described the inertia emulation is implemented. The gains K_p and K_d in figure 8 are increased from 1-15, the system is linearized and the eigenvalues shown in table 1 are calculated. The result shows that only the $0.875Hz$ mode is affected by the synthetic inertia emulation. The eigenvalue corresponding to the $0.875Hz$ mode is presented in table 2. This table shows a weak decrease in the damping of the $0.875Hz$ mode.

$[Kp, Kd]$	$\lambda_{10,11}$	Damping
$[1, 1]$	$-0.42 \pm 5.48i$	0.0758
$[2, 2]$	$-0.41 \pm 5.48i$	0.0754
$[4, 4]$	$-0.41 \pm 5.48i$	0.0749
$[6, 6]$	$-0.40 \pm 5.48i$	0.0736
$[10, 10]$	$-0.39 \pm 5.48i$	0.0718
$[15, 15]$	$-0.38 \pm 5.48i$	0.0701

Table 2: Damping of$0.88Hz$ mode with different amounts of inertia.

However, there are nonlinearities in the system which are not taken into account in the linearized model. Particularly figure 9 on page 15 illustrates a higly nonlinear effect which offers a challenge for the inertia emulation. When changing the turbine speed, the tip speed ratio is also changed, which causes a decreased coefficient of performance. When drastic amounts of inertia are extracted from the turbine, the aerodynamical torque may be reduced to such a level that the turbine speed never recovers. With the load connection of 600MW at bus 3, and K_p and K_d of 15, this situation occurs.

Figure 25 illustrates this situation. The aggressive inertia emulation after the disconnection reduces the rotational speed of the turbine, leading to a collapse in the coefficient of performance. As the inertial response is proportional both to the frequency deviation and its derivative, the key to this problem is the proportional term. This is because the proportional term increases the power reference to the inverter as long as the frequency deviates. However, figure 25 also shows that the inertial response from the wind farm (P:G2) is much larger than the response from the synchronous generator of equal size (P:G4).

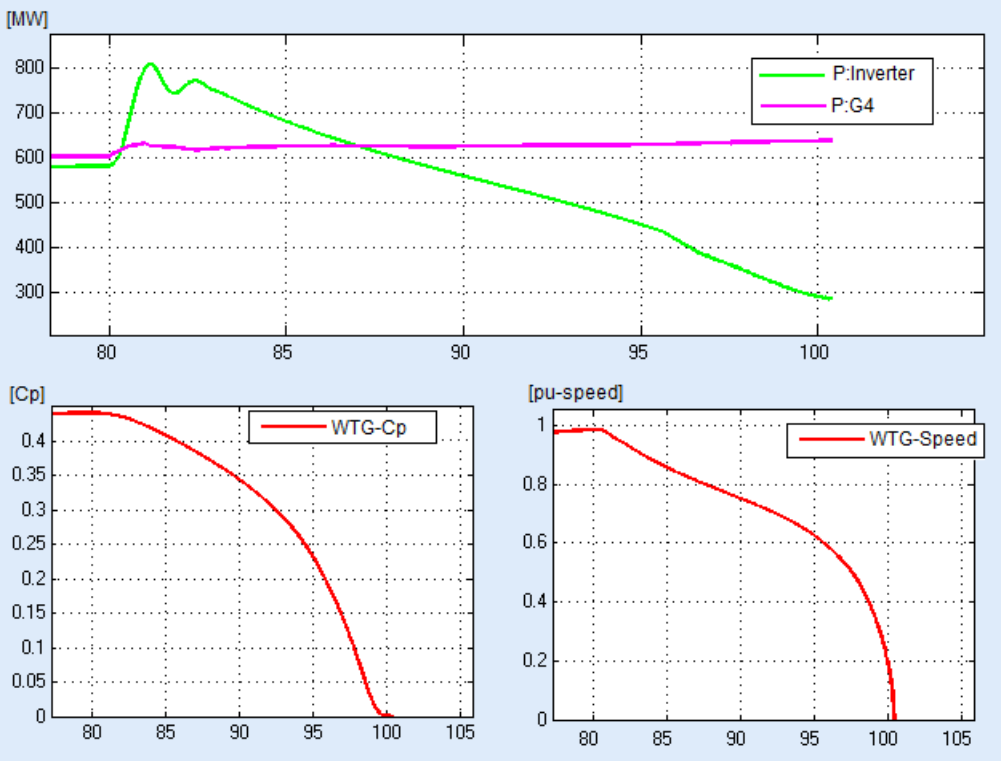

Figure 25: Aggressive inertia emulation leads to collapse in coefficient of performance.

The problem illustrated in figure 25 is created because the wind farm contributes, not only to the inertial response, but also to the primary frequency regulation, but without any other energy storage than the inertia. This is due to the proportional gain in the inertia controller, which increases the power reference while the frequency is deviating from the nominal value. This leads to the idea that the system would benefit if the derivative gain in the controller was dominating.

Separately increasing inertia controller gains

Table 3 and 4 show how the eigenvalues corresponding to the $0.88Hz$ mode change as the derivative and proportional gains are changed separately, while the other is kept constant at 1. The sensitivity analysis is only focusing on the $0.88Hz$ mode as the $2.3Hz$ mode is not affected by the inertial response

in the inverter. This is because the $2.3Hz$ mode corresponds to the oscillation between G3 and G4, not affected by these changes in the other area. The tables illustrate that the damping is not changed while the derivative gain is changed. However, as the proportional gain is increased, the damping clearly becomes worse. It should be noticed that even though 0.5% decrease in damping may not seem much, the decrease is due to changes in one single small unit, only representing 6% of the generation in the system. Therefore, the values chosen for the inertia controller are 1 for the proportional gain and 8 for the derivative gain.

$Kp, Kd =$	$\lambda_{10,11}$	Damping
1,1	$-0.416 \pm 5.48i$	0.0758
1,2	$-0.417 \pm 5.48i$	0.0758
1,4	$-0.417 \pm 5.48i$	0.0758
1,8	$-0.417 \pm 5.48i$	0.0758
1,12	$-0.417 \pm 5.48i$	0.0758
1,15	$-0.418 \pm 5.48i$	0.0759

Table 3: Changes in damping of$0.88Hz$ mode with derivative gain.

$Kp, Kd =$	$\lambda_{10,11}$	Damping
1,1	$-0.416 \pm 5.48i$	0.0758
2,1	$-0.414 \pm 5.48i$	0.0754
4,1	$-0.409 \pm 5.47i$	0.0746
8,1	$-0.399 \pm 5.46i$	0.0730
12,1	$-0.389 \pm 5.44i$	0.0714
15,1	$-0.382 \pm 5.43i$	0.0703

Table 4: Changes in damping of$0.88Hz$ mode with proportional gain.

4.3.2 Changes in other parameters in the inverter

Filter time constant

There are seven other parameters one could change in the inverter controller. Of these seven, four are considered to be constant, these four are the switching time delay and the tuning of the current PI controllers. The remaining three parameters are the power and voltage PI-controllers and the time constant

in the low pass filter, representing the time delay in frequency measurement. Table 5 shows how the eigenvalues are affected by changing the filter time constant from $20ms$ to $1s$. The filter time constant corresponds to T_{del} in $\frac{1}{1+sT_{del}}$. Clearly table 5 shows that the damping of the eigenvalues are not affected by changes within the filter time constant. However, a filter time constant of 1 second will make the reaction from the inertia controller slow and to a large degree limit the output of the derivative gain, which again would lead to very little inertial contribution.

T_{del}[s]	$\lambda_{10,11}$	Damping
0.02	$-0.417 \pm 5.48i$	0.0758
0.05	$-0.417 \pm 5.48i$	0.0758
0.1	$-0.417 \pm 5.48i$	0.0758
0.5	$-0.418 \pm 5.48i$	0.0760
1	$-0.419 \pm 5.48i$	0.0762

Table 5: Changes in damping of $0.88Hz$ mode with filter time delay.

Power and voltage PI-controllers

The other parameters to be examined are the tuning of the PI-controllers, controlling the power and voltage in the inverter. They are the blocks named "Power" and "Voltage" in figure 13 on page 21. These two parameters largely influence the damping of the electromechanical eigenvalues as figure 26 and table 6 illustrate. For simplicity the tuning of the two controllers are identical. In eralier simulations the tuning corresponds to the green circles in figure 26, with $[P, I] = [10, 5]$ in the controller equation $u(t) = P\varepsilon(t) + I\frac{1}{s}\varepsilon(t)$ where $u(t)$ is the controller output and $\varepsilon(t)$ is the deviation from the reference.

When the PI-tuning is changed, the damping of the $0.88Hz$ mode is to a large degree influenced. The eigenvalues indicate that the slower the power/voltage controllers are in the inverter, the better is the damping of the inter-area oscillation. This can clearly be seen as the negative real part of the eigenvalues corresponding to the $0.88Hz$ mode increases as the tuning becomes less aggressive. The $2.34Hz$ mode is hardly not affected, but it is possible to observe a slightly improved damping.

However, a "new" mode approaches the stability limit. Figure 26 shows

this mode for the two least aggressive controller settings. This mode is the oscillation between the inverter and the closest generator (G1), and can be considered to be the equivalent of the oscillation between G3 and G4. This mode has not been noticed earlier because of high frequencies and good damping. As the controllers are less aggressively tuned, this mode becomes slower and more poorly damped.

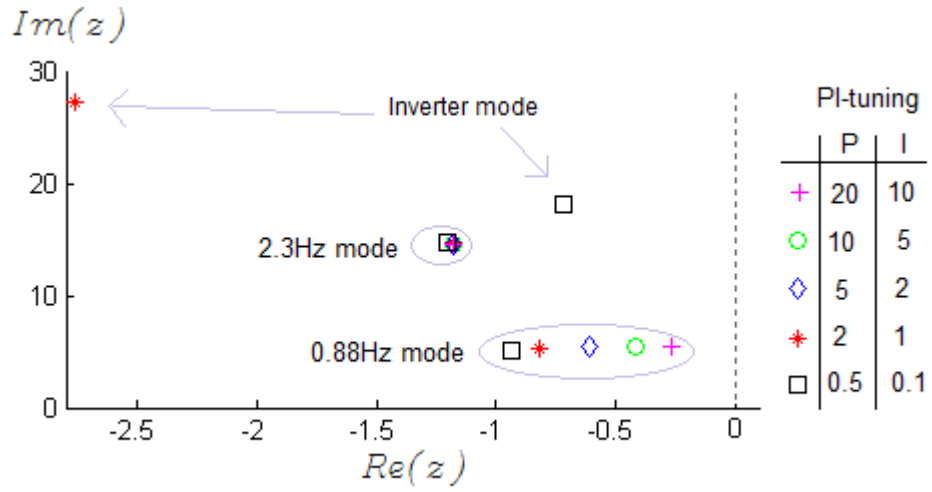

Figure 26: Electromechanical eigenvalues with different PI-tuning of the power and voltage controllers in the inverter.

	Damping of modes			frequency of
PI-tuning [P,I]	0.88Hz mode	2.3Hz mode	Inverter mode	inverter mode
[20,10]	4.77%	8.02%	22.8%	$20.7Hz$
[10,5]	7.58%	8.03%	19.7%	$11.7Hz$
[5,2]	11.0%	8.03%	16.7%	$7.1Hz$
[2,1]	14.9%	8.06%	10.1%	$4.35Hz$
[0.5,0.1]	18.1%	8.14%	3.94%	$2.91Hz$

Table 6: Damping of modes to different PI-controller tuning.

The effect of these changes are presented in figure 27. The left column of graphs corresponds to the basic PI-controller settings; $[P, I] = [10, 5]$. The right column corresponds to a controller tuning with $[P, I] = [0.5, 0.1]$. It

should be noticed that the graphs show two different events; the first figure illustrates the ability of the inverter to follow a power reference with a step change in power reference from 0.6 to 0.65. The two other graphs show the behavior during a simulated fault at bus 3. The two different graphs illustrate how the eigenvalues are affected by the controller tuning. The black line in the lowest graph corresponds to the power transmitted between the two areas, here the inter-area oscillation of $0.88Hz/0.82Hz$ is clearly visible. With a weak controller in the inverter, the improved damping of this oscillation is significant, even though the inverter is relatively small compared to the rest of the area. However, the weak controller leads to a poorly damped $2.9Hz$ oscillation, henceforth named the "inverter mode". The suggested tuning for the controllers is $[P, I] = [2, 1]$. This tuning provides improved damping of the inter-area mode, while the inverter mode is still well damped.

4.3.3 Impact on critical clearing time.

The "sensitivity" analysis on critical clearing time is performed with a fault at bus 3. The fault is modeled as a 0.01p.u. resistance, where the impedance base is 176.4Ω in the 1000MVA/420kV based system. The critical clearing time presented is the last millisecond of fault duration before the synchronism is lost and the system becomes unstable. Table 7 shows how the critical clearing time of a fault on bus 3 is affected by the tuning of the inertia emulation parameters for different inertia constants in G1. From the table, two main observations can be obtained. The inertia constant of G1 has a significant impact, and the inertia emulation gives a slight decrease in critical clearing time. It should be noticed that fault ride through capability is an important topic in inverter design and this inverter model does not include such features.

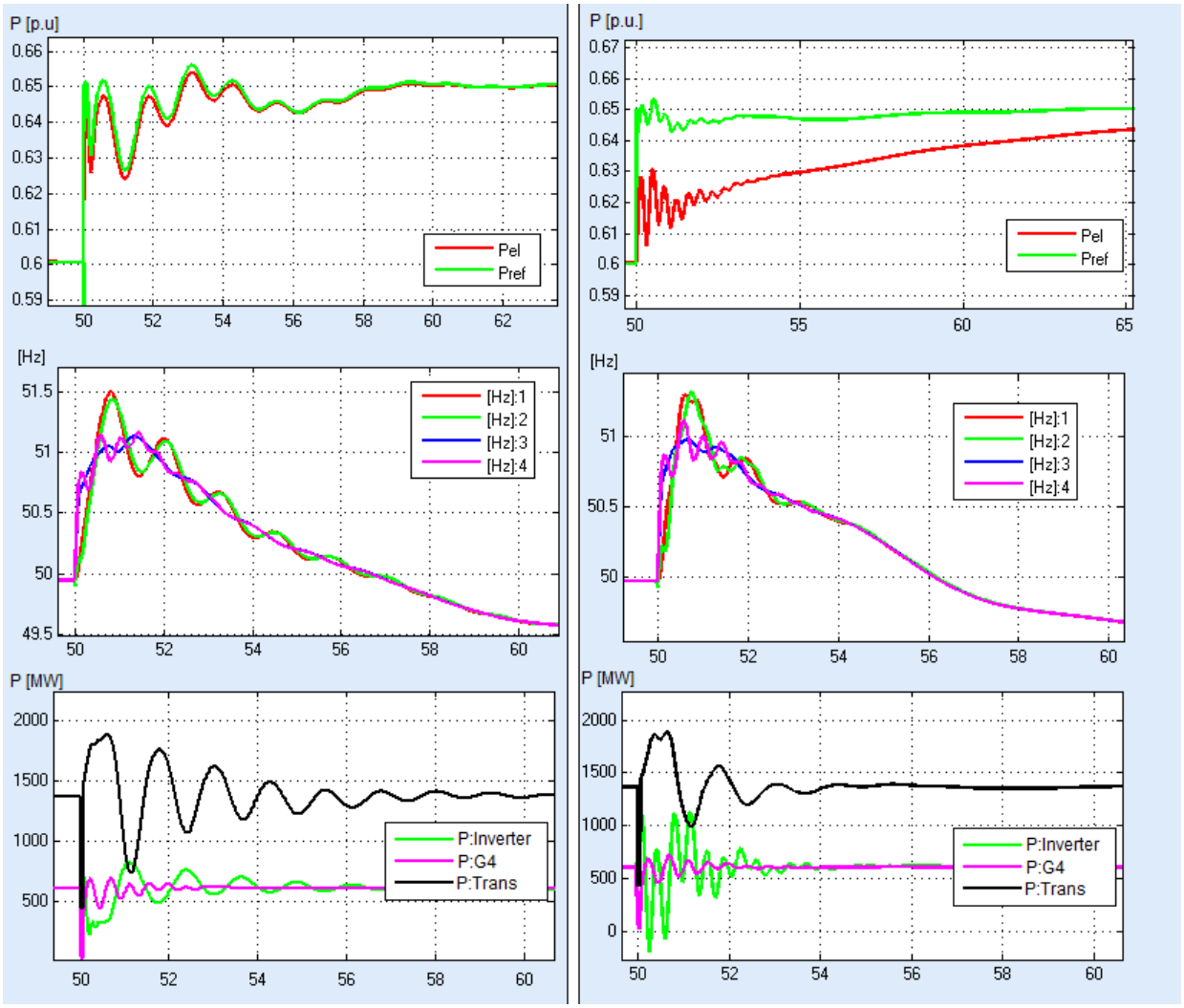

Figure 27: Corresponding events with different controller tuning. Left; $[P, I] = [10, 5]$. Right; $[P, I] = [0.5, 0.1]$.

Inertia tuning		Inertia constant in G1		
Proportional, Kp	Derivative, Kd	$H_1 = 3s$	$H_1 = 4.5s$ (value in base case)	$H_1 = 6s$
0 (No inertia)	0 (No inertia)	225ms	162ms	126ms
1	2	215ms	156ms	121ms
1	4	210ms	151ms	118ms
1	8	208ms	148ms	114ms
1	12	208ms	149ms	113ms
2	1	218ms	158ms	122ms
4	1	216ms	156ms	120ms
8	1	215ms	152ms	117ms
12	1	211ms	149ms	114ms

Table 7: Table of critical clearing time for a fault at bus 3 for different parameter tuning of synthetic inertia.

Table 8 shows how critical clearing time is affected by changing the power/voltage PI-control parameters. Here, the inertia controller is set with a proportional gain of 1 and a derivative gain of 8, while the inertia constant in G1 is $4.5s$. The trend in the table indicates that the critical clearing time is decreased with a more aggressive controller setting. Figure 28 illustrates the first oscillations after a fault with controller tuning $[P, I] = [2, 1]$. The large response in voltage angle at bus 1 and 2 is an expression for the oscillations between the areas, as the angular reference is the rotor position at G3. It should also be noticed that even though the fault is at bus 3, the ability to provide electric power is more deteriorated at G1 during the first swing. This may be due to the influence from the inverter.

P	I	$T_i = P/I$	Critical clearing time
10	5	2s	141ms
5	2	2.5s	143ms
2	1	2s	148ms
2	0.2	10s	151ms
0.5	0.1	5s	171ms

Table 8: Table of critical clearing time for a fault at bus 3 for some different power/voltage control parameters.

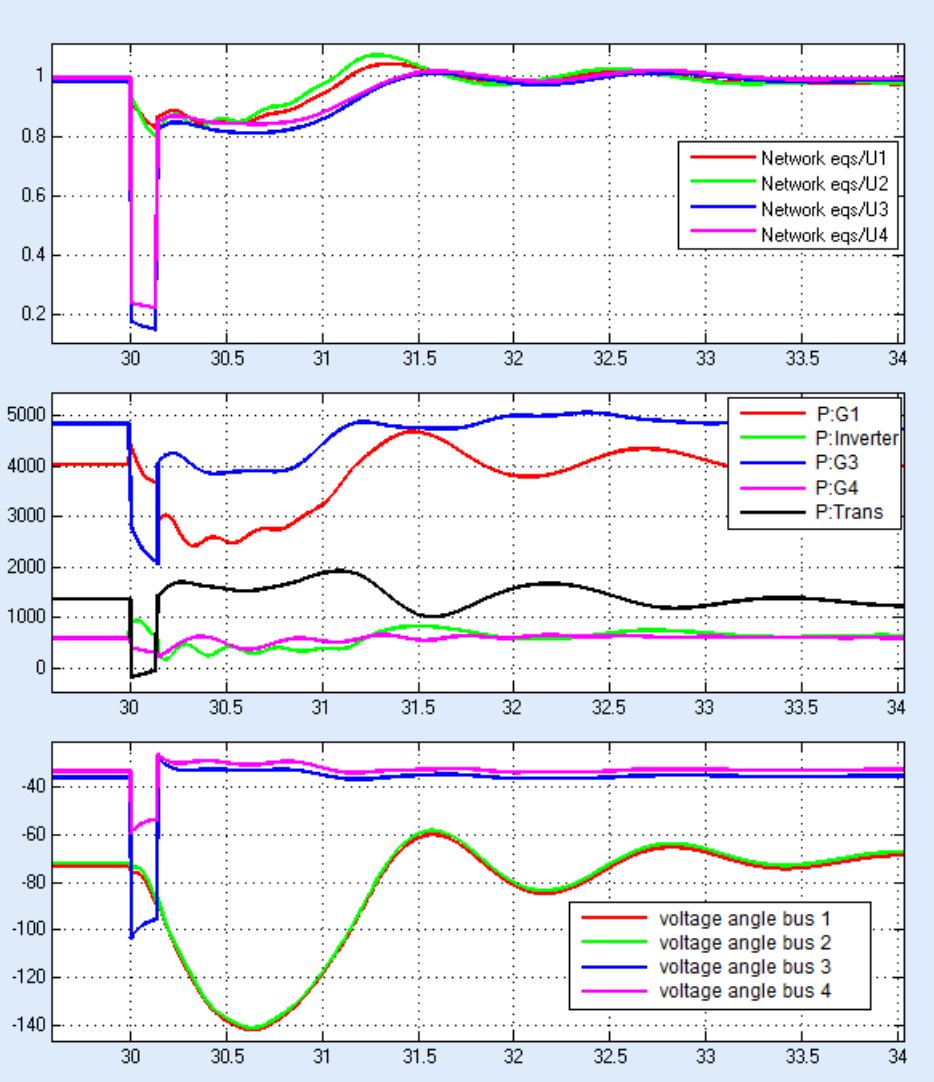

Figure 28: The first swing after fault.

4.4 Suggested tuning and inertial response

From the simulations above one may obtain a suggested tuning. It is suggested that the inertia controller should be dominated by the derivative term. This is because the proportional gain gives a negative effect on the damping of the inter area mode and risks to provide too much inertia over time,

possibly creating a collapse in the coefficient of performance. The suggested tuning is $[K_d, K_p] = [8, 1]$.

Although the simulations show that the critical clearing time is affected by the inertia emulation, it is not considered a major issue as the fault ride through capability of the inverter is assumed not sufficiently modelled. The power/voltage PI-controllers give a major impact on the damping of the inter area mode, and also influence the critical clearing time. Here, the proportional and integral gains are suggested $[P, I] = [2, 1]$, which provide sufficient damping for both the inverter mode and the inter area mode.

The filter time constant for frequency measurement turned out to be less important for the damping of modes in the linearized system. However, it has major influence upon the inertial response. A filter time constant of $0.1s$ is suggested in the model. A too small measurement time delay is problematic if the derivative term in the inertia emulation controller is large.

Also the PI-controllers in the current controllers need to be closely tuned with the switching time delay. In the model the switching time constant is assumed to be 2ms. This corresponds to a switching frequency of $250Hz$ in the inverter. The current controller tuning is then $[P, I] = [0.005, 0.0005]$. These values need to be small in order for the model to be stable, and there is only a tiny "window" where the model is stable.

Figure 29 can be compared to figure 22 on page 35 and illustrates the inertial response from the inverter after a load connection at bus 1. The load increase is ramped from 0-600 MW in 1 second. The inverter contributes with more inertia than the synchronous generator the first few second but then reduces the power output. This is considered positive, as the response is desired to be inertial to give the primary controllers in the system time to respond to the falling frequency.

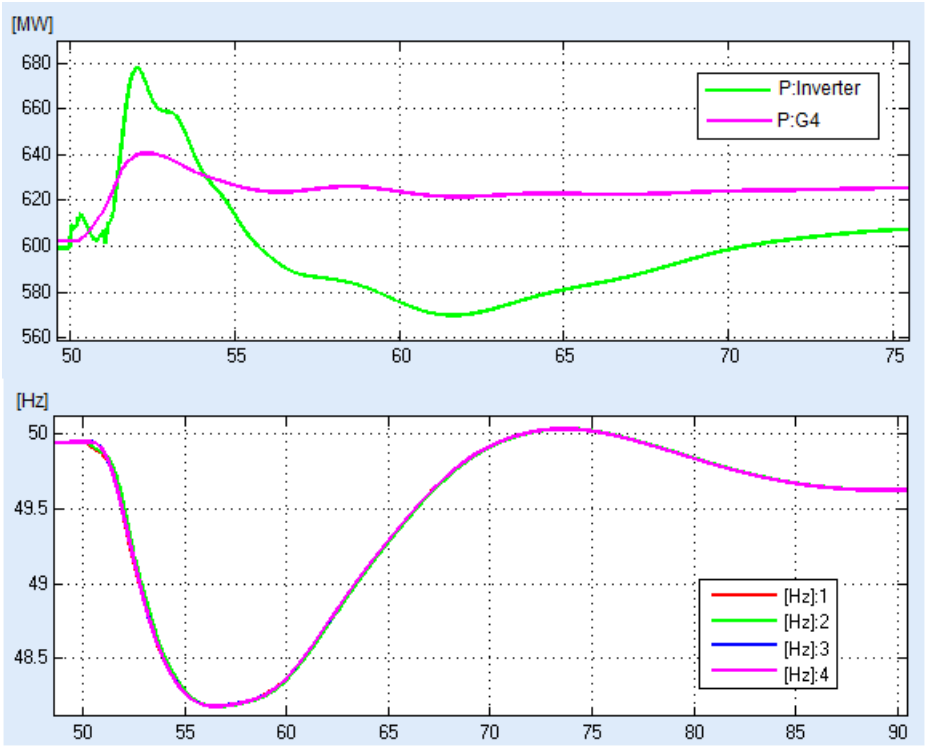

Figure 29: Inertial repose, 600 MW load connection at bus at bus 1.

If closely examined, it can be seen that the inertial response from the wind farm provides a slightly slower rate of change in frequency the first seconds after the connection. It is only a marginal improvement because the inverter is only 6% of the system size. It can also be noticed that the time before recovery is slightly increased. These are the two main impacts synthetic inertia is known to provide in governor based simulations [8][9].

5 Discussion

5.1 Impacts on rotor angle stability

The sensitivity analyses has focused on the controller tuning in the inverter and its impact on the electromechanical eigenvalues. Here there are two main focus areas; the amount of inertial contribution, and the rapidness of the inverter. The inertial contribution is determined by the two gains, named proportional and derivative gain, in the inertia controller. The rapidness of the inverter is controlled by the two PI controllers for power and voltage control, giving set points for the active and reactive current. When the impact on system stability is studied it should be emphasized that the relative size of the inverter is 6% of the system. Therefore, all changes in system stability are considered interesting.

By changing the two control parameters for the inertial response it was observed that they had a minor influence in the damping of the inter area oscillatory mode. However, the eigenvalue analysis indicated that only the proportional gain had a negative impact on the damping. When increasing the proportional gain from 1 to 12, keeping the derivative gain constant at 1, the damping of the inter-area mode was reduced from 7.6% to 7%. On the other hand, when the derivative gain was increased and the proportional gain kept constant, the damping was approximately constant with a marginal increase in damping.

This is an argument for letting the derivative gain dominate the inertial controller. Generally, the purpose of the proportional gain is to keep the inertial contribution positive when the grid frequency is at its lowest and to provide additional time before the delivered inertia is "drawn back" from the grid. In other words the purpose of the proportional gain in the inertia controller approaches primary frequency control. This is a dangerous landscape to enter without another energy storage than the inertia as the coefficient of performance may collapse.

By changing the PI-tuning in the power and voltage controllers, a major impact on the system modes was observed. Generally for a system of n synchronous generators there would be $n-1$ electromechanical eigenvalues, with frequencies in the range of $0.2-2Hz$. Normally the frequency

and damping of these modes will to a certain degree depend on rotational mass, impedance relations and voltage. In the first simulations, the inverter mode was neglected, as it was well damped and very fast (20% damping at $12Hz$). When the power/voltage controllers in the inverter were tuned, this mode was changed drastically. From table 6 on page 42 it is observed that an aggressive controller gives a well damped, fast oscillating inverter mode. However, this also resulted in a poorly damped inter area mode. It seems that the power/voltage controllers need to be tuned, compromising between damping of inter the area mode and the ability to follow the power reference. It should also be noticed how drastic the damping of the inter area mode was affected by the tuning of the power/voltage controller. In the tested tunings the damping of this mode varies from 4.7-18%! In this specific case the compromise seemed to work out fine, but as the tuning of the inverter largely influences the damping of the inter area mode, this may be an issue for more complex grid topologies when power electronics becomes a significant share of the system size.

5.2 Impacts on critical clearing time

The simulations aim to illustrate how the controller tuning affects the time a fault can be active before the system becomes unstable. The mechanism of becoming unstable can be described relating back to figure 14 on page 23. Assuming the system initially operates very close to the equilibrium point, when the disturbance is applied the operating point starts to move away from the equilibrium point in the state space. At some point at time $t = t_{cct}$ the distance from the equilibrium point is η and hence the system does not remain stable.

The simulations indicate that the critical clearing time is reduced when the inverter is providing synthetic inertia. The impact is not large, but absolutely noticable. Impact on critical clearing time from different tuning in the power/voltage controllers was also studied, and indicates that the critical clearing time is reduced if the controllers are more aggressive. However, there are weaknesses in the model when it comes to this topic. In real inverters there are mechanisms to improve the fault ride through capability, and more limitations than what the present model provides. This is seen in rather unrealistic responses when the fault is moved closer to the inverter. The model seems best suited for small signal stability, when the inverter operates within

linear conditions.

Even though the model has weaknesses when it comes to handle large disturbances, it is interesting that no matter how the inertia relation is between the two areas, the area with the inverter is clearly has the worst response. It may seem like the rapid dynamics of the inverter influences the voltage angle at synchronous generator bus and affects the generator ability to provide electric torque in the first swing.

5.3 Inertial contribution

The potential inertial contribution is considered to be significant. As figure 29 illustrates, the inertial response can exceed that of a synchronous generator of equal size. This contribution may become important in power systems with a large share of inverter interfaced generation capacity. However, it is important to keep the response inertial, and not to provide primary frequency regulation without a spinning reserve. This is performed by letting the derivative gain in the inertia controller dominate over the proportional gain. In this way the response is acting mostly towards limiting the rate of change in frequency, not the actual frequency deviation.

A little discussed issue in these simulations is the fact that the amount of inertia varies with the wind speed. The inertia of a synchronous generator is fixed due to the synchronous speed, however, a variable speed wind turbine varies the speed and also the stored inertia. This is an important issue because the speed of the turbine is the square of the wind speed in per unit values. Combined with increased sensitivity of tip speed ratio at lower rotational speeds, the amount of inertia that can be delivered is drastically reduced with lower wind speeds. However, the need for synthetic inertia will be at its largest when the power system has a huge share of wind generation, hence the problem from a TSOs point of view may solve itself.

Another little discussed issue is the actual inertia of a wind turbine. This is also a very important parameter for the amount of inertia delivered to the grid. A lighter turbine will decelerate faster and reduce the power set point more rapidy, also increasing the risk of a collapse in coefficient of performance. In the simulations the inertia constant is assumed to be $H_{wtg} = 5s$, relating back to the swing equation, equation 2 on page 5. Calculations found

in literature [10] suggest the inertia constant for a 2MW wind turbine to be $4.79s$, so the assumption seems to be inside the scope. However, wind turbines are made to be as light as possible and the amount of inertia possible to be extracted may become lower with increased power ratings and material development.

6 Conclusion

Inertial contribution from synthetic inertia in wind turbines is considered to be the solution to provide inertia in a power system with significant amounts of inverter interfaced power generation. The main advantage seen from the frequency stability point of view is that the rate of change in frequency is limited following a disturbance. Generally synthetic inertia makes the frequency response slower, providing a slower change during the primary frequency response, but also increasing the time before frequency recovery.

The main topic in this project has been to find out if the transient stability and oscillation damping in the system was affected by the utilization of synthetic inertia. The eigenvalue analysis indicates that the phase of the inertial response is the key to determine if the damping is negatively affected. By letting the derivative gain dominate the response, the damping was not negatively affected. However, if the proportional gain dominated, the damping of the inter area mode was reduced. Letting the derivative gain dominate the response will reduce the risk of a collapse in the coefficient of performance, as a large proportional gain acts as a contributor to the primary frequency regulation.

The eigenvalue analysis also indicates that the rapidness of the inverter controller has a major impact on the oscillation damping in the system. Generally a "stiff" inverter, with very aggressive controllers gave a very stable inverter mode, however the inter area mode became poorly damped. On the other hand a "slack" inverter with less aggressive controllers gave a slower less damped inverter mode, but increased the damping on the inter area mode. For this topology a good compromise was found. However, it is still considered surprising that the influence was so significant even though the relative size of the inverter was small compared to the system size.

Concerning transient stability, impacts on critical clearing time has been studied. The results indicate that synthetic inertia gives a slight deterioration on the critical clearing time. However, the model is considered to be insufficient simulate the behaviour of the inverter during large disturbances as there are fault ride through mechanisms, not included in the model. However, it seems like the response from the inverter to some degree deteriorates the stability in the closest generator by affecting the voltage angle at its ter-

minals.

And so, the all over conclusion is that implementing synthetic inertia alone does not largely influence the damping of the system as long as the inertia controller is tuned "correct". However the inverter controllers need to be carefully tuned to obtain a well damped system. These issues were the main objectives in the project.

7 Recommendations for further work

7.1 Suggested model improvements

The model is considered to be sufficiently detailed to give an impression of the impact on the system stability when synthetic inertia is implemented in an existing power system. However, there are improvements in the model to provide a higher level of accuracy.

Load model

Perhaps the most significant improvement would be to provide a better load model, as the present one is a constant impedance model. Generally, it is said that a constant impedance load is far less challenging that a constant power load. This would require a block that takes the bus voltage as input and uses a script to calculate the "seen" impedance. This kind of load would create more stability challenges. A parallel can be drawn to the PI controller tuning in the power and voltage control in the inverter. Here the inter area oscillation turned out to be poorly damped when the inverter rapidly followed the power reference. The comparison here is that the rapid inverter can be considered a negative constant power load and hence is difficult for the system to handle.

Saturation models

The effects of magnetic saturation in iron has a large influence on the ability to provide excitation emf. The effect is highly nonlinear and would create more differences between the predicted response from the linearized system and the actual response. The implementation would be to include the saturation function $S_E = f(E_f)$ in the block diagram of the AVR-model shown in figure 3 on page 7.

Network representation and initialization problems

The model is unique in the way that it works for this system, and this system only. If a more general model should be made, two critical issues need to be handled more automatically; the network representation and the state variable initialization. The network representation is modelled as an admittance matrix in the main script. There are several disadvantages in this

representation. The admittance matrix in the 4-bus system is a 4x4 matrix with many complex numbers and many possible typing errors. A slight error in this matrix effectively destroys the entire model. As the matrix is manually made, this is a large source of errors. A large improvement would be to use a script to declare the impedance relations in the system and then have a script to build the admittance matrix and export it to the model. This would however, make the constant power load model more difficult to implement. Also, the model would be more user friendly if the most critical state variables could be initialized in a more user friendly way. However, the initialization of state variables requires a valid load flow situation.

Fault ride through mechanisms

The inverter model shows a poor ability to remain stable after a short circuit. In the critical clearing time studies, the fault is at bus 3, hence there is a relatively large impedance between the inverter and the fault. This is seen in the post fault voltage which, even during the fault, is seldom less that $0.8p.u.$ This illustrates the inverter models poor ability to maintain stable during a fault. However, actual inverters are equipped with fault ride through mechanisms which are not modeled in this project. These mechanisms could be interesting to include as a model improvement.

PSS-models

Power system stabilizer models could be included to improve the accuracy of the model.

7.2 Virtual synchronous generator concept

It is suggested to explore how the inverter controller can be utilized to obtain a virtual synchronous generator. Also how the chosen parameters for the virtual synchronous generator affects the damping of the electromechanical eigenvalues.

8 Appendix

8.1 Linearization issues regarding mode shapes in Simulink/Matlab

When the linearized system is exported to Matlab and the eigenvector matrix is calculated it is important to remember what Matlab considers to be a state variable and what is considered a state variable in power system analysis. Consider the equation for subtransient emf in d-axis, equation 6 on page 6.

$$T''_{qo}\dot{E}''_d = E'_d - E''_d - I_q(x'_q - x''_q)$$

The state variable in power system analysis would be E''_d. Implemented in Simulink the model will look like figure 30. Remember that in the fifth order model E'_d is zero. To represent the term $\frac{1}{1+T''_{qo}s}$ a state space model is utilized due to the simplicity regarding initialization of state variables. However, this creates a difference between what matlab sees as a state variable and the "natural" state variable in power system analysis.

Figure 30: Simulink implementation of equation 6 on page 6.

The problem mentioned above can be illustrated by the block diagram of a state space model, shown in figure 31. Our state variable E''_d is now the output of the state space model, marked as y in figure 31, the problem is that the state variable in Matlab is x. This is not a problem in time domain simulations. However, when the linearized system is to be studied, it is important to be aware of this, particularly when creating and interpreting mode shape plots.

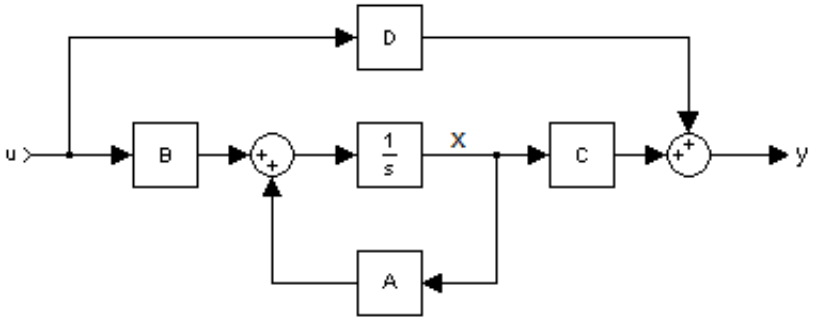

Figure 31: Block diagram of a state space model, figure from Wikipedia [7].

To obtain a "valid" mode shape plot the states one chooses need to be picked carefully, but a valid mode shape plot gives important information about the oscillatory behavior of the system. There are three things that can be obtained from the mode shapes; phase angles, relative magnitude, and actual magnitude (if the eigenvector elements are not normalized). Here follows some information about which states that provide mode shape plots that are easy to interpret.

- States that are represented by a pure integration, such as angular displacement, δ, and speed deviation, $\triangle\omega$ are the most intuitive to use for mode shapes. Considering the state $\triangle\omega$ mode shapes can be obtained for all synchronous generators. However, speed deviation occurs as two different values in the model, deviation from reference speed and deviation from system reference speed. To obtain a valid mode shape plot the state variable in all generators need to be the deviation from reference speed. The other variable, deviation from system reference speed, integrates up to angular displacement, δ. The state variable δ can be used to create mode shapes without any problems. However, the reference generator does not have this state variable because the variable represents the angular displacement from the q-axis of the reference generator.

- State variables in state space models where C (in figure 31) are equal. In the model all the generators utilize the same AVR-model, hence the excitation emf is a variable well suited for mode shapes. If all the generators are assumed to have the same open circuit time constant, $E_q^{'}$

could also give valid mode shape plots. However, these time constants are not assumed to be equal.

- It is difficult to find states in the inverter that can be utilized in mode shapes for comparison with synchronous generator states. The inverter state variables $E_{q,sys}$ and $E_{d,sys}$ represents the emf directly related to the system reference frame. The magnitude of this emf oscillates with the system voltages, however, as the states relate to the system frame, each of the states oscillates in close relation to δ in the closest synchronous generator. Unfortunately the gain (C) in the state space model representing the inverter emfs is very large, giving large differences in the "physical" state variable, and the Matlab-state variable. The frequency measurement filter in the inverter model includes a state that translates into frequency deviation, which should be directly the same as the speed deviation state in the synchronous generators. Therefore, the mode shapes does not "fit" both because of the gain (C) in the state space model, and possibly also affected by the linear approximation to the derivative term in frequency calculation.

8.2 List of symbols and abbreviations

AVR	automatic voltage regulator
AC	alternating current
DC	direct current
IGBT	component: insulated gate bipolar transistor
MOSFET	component: metal–oxide–semiconductor field-effect transistor
MVA	mega volt ampere
MW	megawatt
SRF	system reference frame (dq)
PSS	power system stabilizer
δ_n	angular deviation between q-axis of generator n and q-axis of reference generator
δ_g	power angle, angle between terminal voltage and generaotr emf
$E^{''}$	subtransient emf
$E_d^{''}$	direct axis component of subtransient emf
$E_q^{''}$	quadrature axis component of subtransient emf
$E^{'}$	transient emf
$E_d^{''}$	direct axis component of transient emf
$E_q^{''}$	quadrature axis component of transient emf
E_f	field excitation emf
X_d, $X_d^{'}$, $X_d^{''}$	d-axis synchronous reactance, transient reactance and subtransient reactance
X_q, $X_q^{'}$, $X_q^{''}$	q-axis synchronous reactance, transient reactance and subtransient reactance
x_t, $x^{''}$	transformer reactance, subtransient reactance
I_{gen}	generator current
$I_{d,}I_q$	d- and q-axis component of generator current
ϕ	phase angle of generator current space vector, refered to system reference frame
U_n	voltage at bus n
ω_n	rotational speed of generator n
H	inertia constant
$T_{do}^{'}$,$T_{do}^{''}$	open circuit transient and subtransient time constant in d-axis
$T_{qo}^{''}$	open circuit subtransient time constant in q-axis

Table 9: List of symbols and abbreviations

P_e,$P_{m(ech)}$	electric power, mechanical power
L_f, R_f	Field winding inductance and resistance
Y	network admittance matrix
Q	reactive power
φ	air density
A	rotor area swept by wind turbine
c_p	coefficient of performance
λ	tip speed ratio of wind turbine
β	pitch angle
V	wind speed
f_s	switching frequency of inverter
θ_{PLL}	phase lock loop angle
f, f_{ref}, f_n	frequency, reference frequency, frequency at bus n
K_d, K_p	derivative gain and proportional gain in inertia emulation controller
$\mathbf{x}$,x_n	state vector, state variable n
η, ε	Used in the Lyapunov definition of stability
$\mathbf{x(t)}$, $\mathbf{y(t)}$, $\mathbf{u(t)}$, $\mathbf{z(t)}$	system state variables, output signals, control signals, disturbance signals.
$\mathbf{W}$	eigenvectormatrix of linear system
w_{ij}	element in eigenvectormatrix corresponding to state variable i and eigenvalue j
λ_j	eigenvalue j
$\mathbf{I}$	identity matrix
ξ	relative damping
e^{Λ}	diagonal matrix of eigenvalues
$\mathbf{z(t)}, \mathbf{z_0}$	modal variables, inital modal variables (vector)
$[P, I]$	proportional and integral gain in PI controller $u(t) = P\varepsilon(t) + I\frac{1}{s}\varepsilon(t)$
$\varepsilon(t)$	deviation from reference value in PI controller
S_{E_f}	saturation function

Table 10: List of symbols and abbreviations

8.3 Full model

Top level

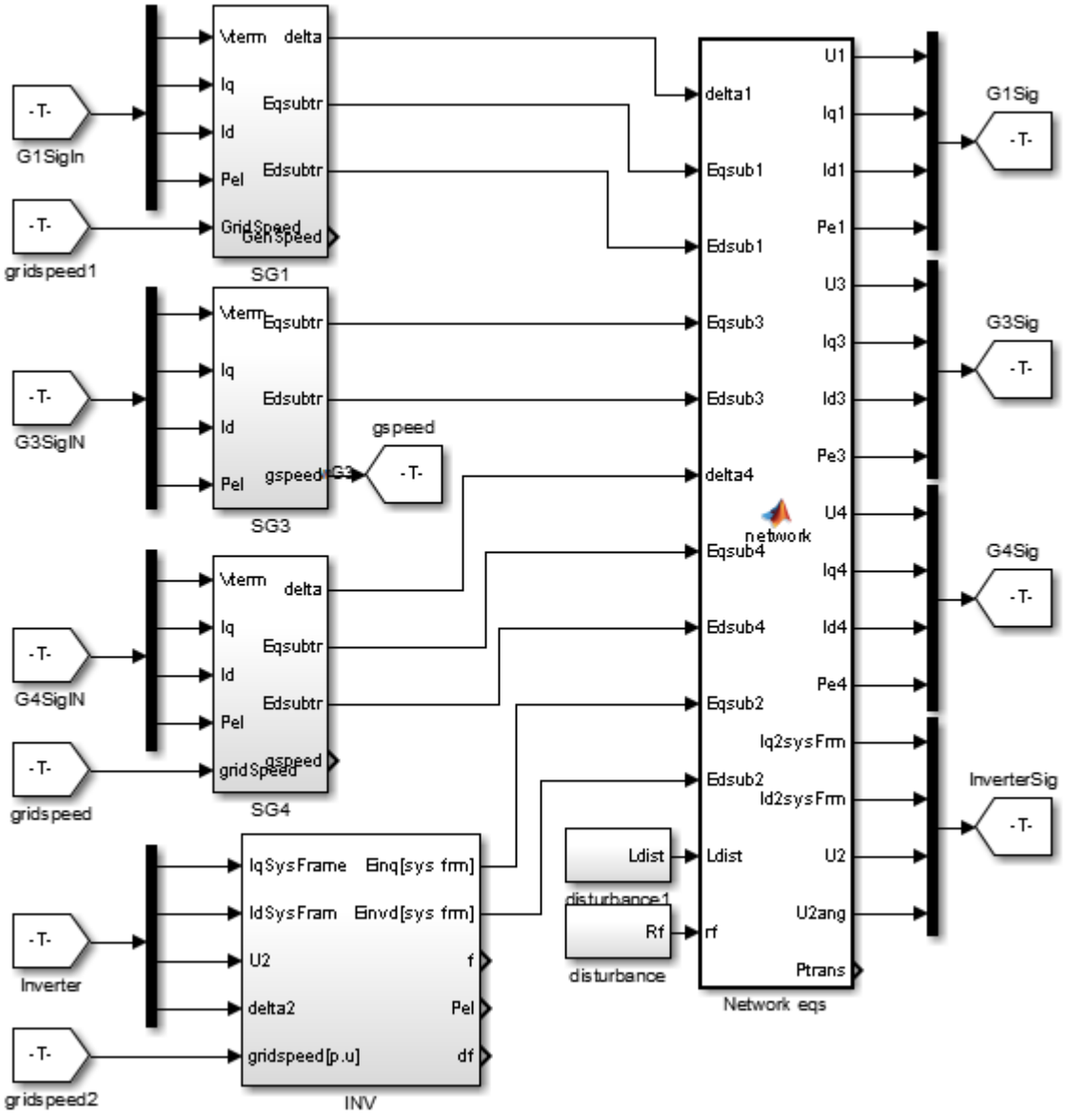

Figure 32: Top level of model.

Network Equation script

```
function [U1,Iq1,Id1,Pe1,U3,Iq3,Id3,Pe3,U4,Iq4,Id4,Pe4,Iq2sysFrm,Id2sysFrm,
    U2,U2ang,Ptrans] = network(delta1,Eqsub1,Edsub1,Eqsub3,Edsub3,delta4,
    Eqsub4,Edsub4,Eqsub2,Edsub2,Ldist,rf)

%Impedance declarations, Ldist is load connection, all values in global p.u
xt1 = 0.02;
xt2 = 0.1;
xt3 = 0.0167;
xt4 = 0.125;

x12 = 0.0363;
x13 = 0.4268;
x34 = 0.0726;

xsub1 = 0.05;
xsub3 = 0.05;
xsub4 = 0.275;

z1 = 1/(6.2-0.1i+Ldist);
z3 = 1/(4.2-0.08i);

%Network representation, admittance matrix, Rf is fault impedance.
Y = [(1/(1i*(xt1+xsub1))+1/z1+1/(1i*x12)+1/(1i*x13)) -1/(1i*x12) -1/(1i*x13) 0;
    -1/(1i*x12) (1/(1i*x12)+1/(1i*xt2)) 0 0;
    -1/(1i*x13) 0 (1/(1i*x13)+1/(1i*x34)+1/z3+1/rf+1/(1i*(xt3+xsub3))) -1/(1i*x34);
    0 0 -1/(1i*x34) (1/(1i*x34)+1/(1i*(xt4+xsub4)))];

%Relating all emfs to system reference frame
E3=Eqsub3+1i*Edsub3;
E1=Eqsub1*cos(delta1)+Eqsub1*sin(delta1)*1i + Edsub1*cos(delta1)*1i-Edsub1*sin↙
(delta1);
E4=Eqsub4*cos(delta4)+Eqsub4*sin(delta4)*1i + Edsub4*cos(delta4)*1i-Edsub4*sin↙
(delta4);
E2=Eqsub2+1i*Edsub2;
```

Figure 33: Algebraic equations 1/3

```
%Current injection model
I01=E1/(1i*(xsub1+xt1));
I02=E2/(1i*xt2);
I03=E3/(1i*(xsub3+xt3));
I04=E4/(1i*(xsub4+xt4));
I=[I01;I02;I03;I04];

%Calculate bus voltges
U=Y\I;
U01 = U(1);
U02 = U(2);
U03 = U(3);
U04 = U(4);

%Voltage represented by magnitude and phase angle (rel to sys frame) -
%notice that only phase angle of inverter are used.
U1 = abs(U01);
U2 = abs(U02);
U3 = abs(U03);
U4 = abs(U04);
```

Figure 34: Algebraic equations 2/3

```
U1ang = angle(U01);
U2ang = angle(U02);
U3ang = angle(U03);
U4ang = angle(U04);

%Generator current calculation
I1gen=(E1-U(1))/((xsub1+xt1)*1i);
I2gen = (E2-U(2))/(1i*xt2);
I3gen =(E3-U(3))/((xsub3+xt3)*1i);
I4gen=(E4-U(4))/((xsub4+xt4)*1i);

%Generator current represented in its own dq-ref frame
Iq1 = abs(I1gen)*cos(delta1-angle(I1gen));
Id1 = -abs(I1gen)*sin(delta1-angle(I1gen));

Iq2sysFrm = abs(I2gen)*cos(-angle(I2gen));
Id2sysFrm = -abs(I2gen)*sin(-angle(I2gen));

Iq3 = abs(I3gen)*cos(-angle(I3gen));
Id3 = -abs(I3gen)*sin(-angle(I3gen));

Iq4 = abs(I4gen)*cos(delta4-angle(I4gen));
Id4 = -abs(I4gen)*sin(delta4-angle(I4gen));

%Electric power calculated for SGs.
Pe1 = Edsub1*Id1+Eqsub1*Iq1;
Pe3 = Edsub3*Id3+Eqsub3*Iq3;
Pe4 = Edsub4*Id4+Eqsub4*Iq4;
```

Figure 35: Algebraic equations 3/3

Synchronous Generator model

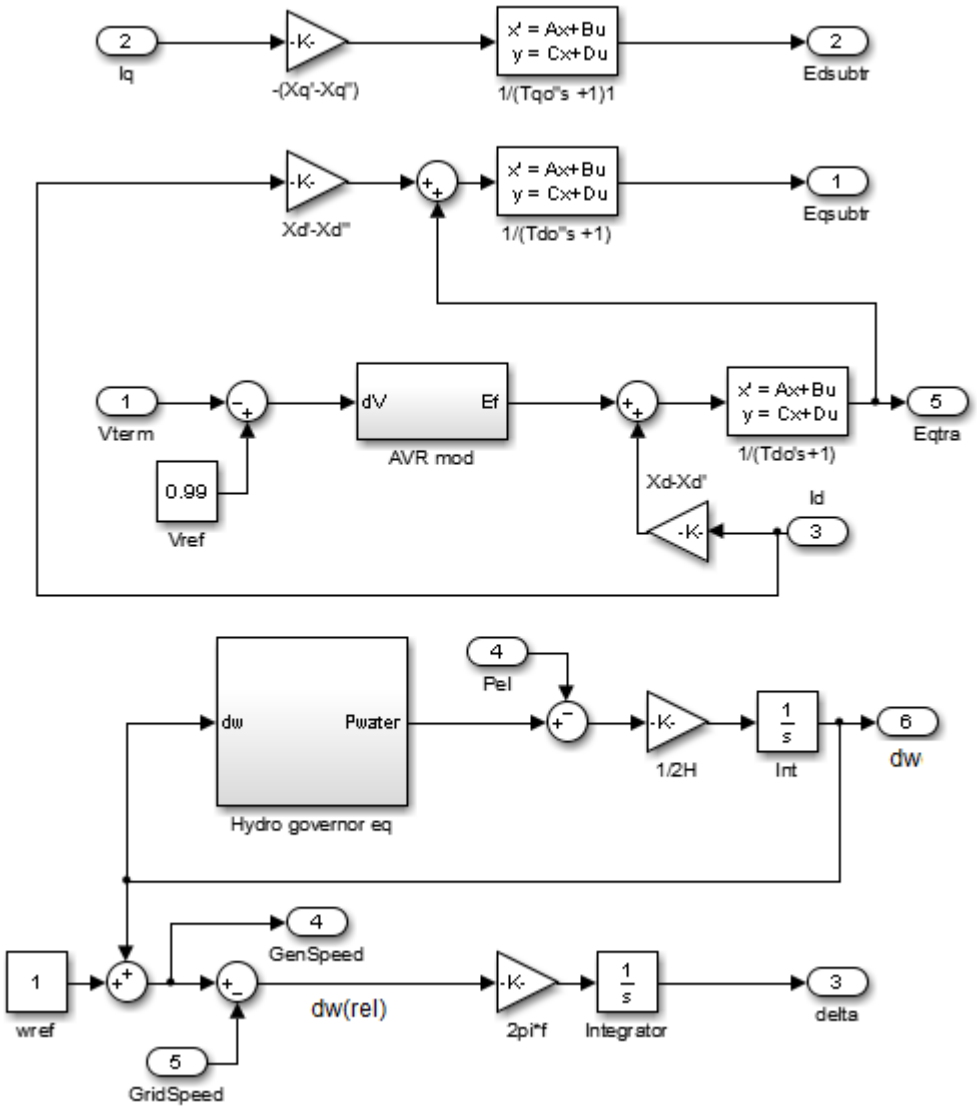

Figure 36: Synchronous generator model

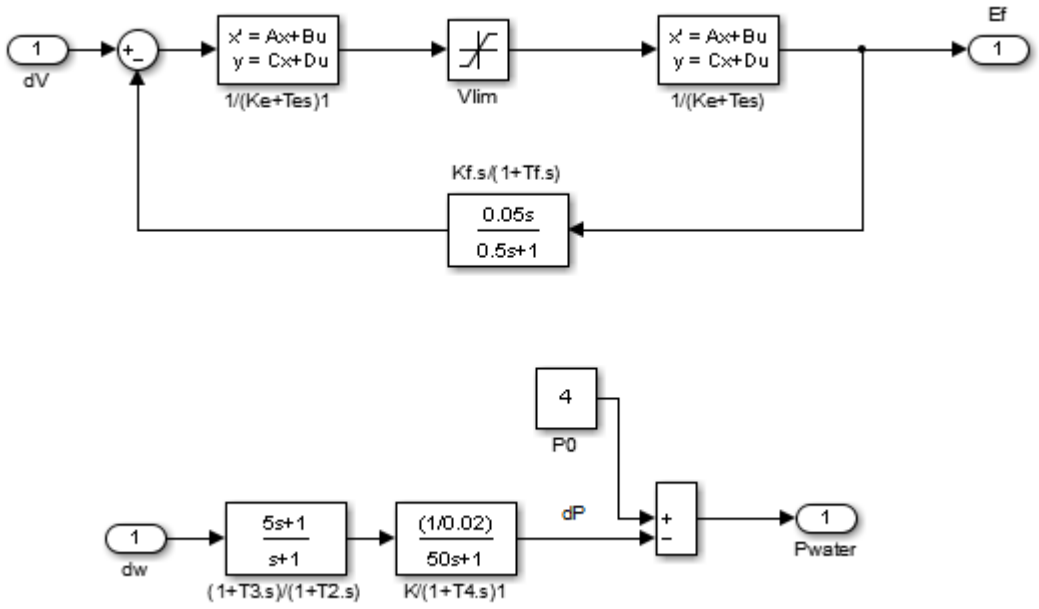

Figure 37: Top: AVR model. Bottom: Governor model.

Inverter model

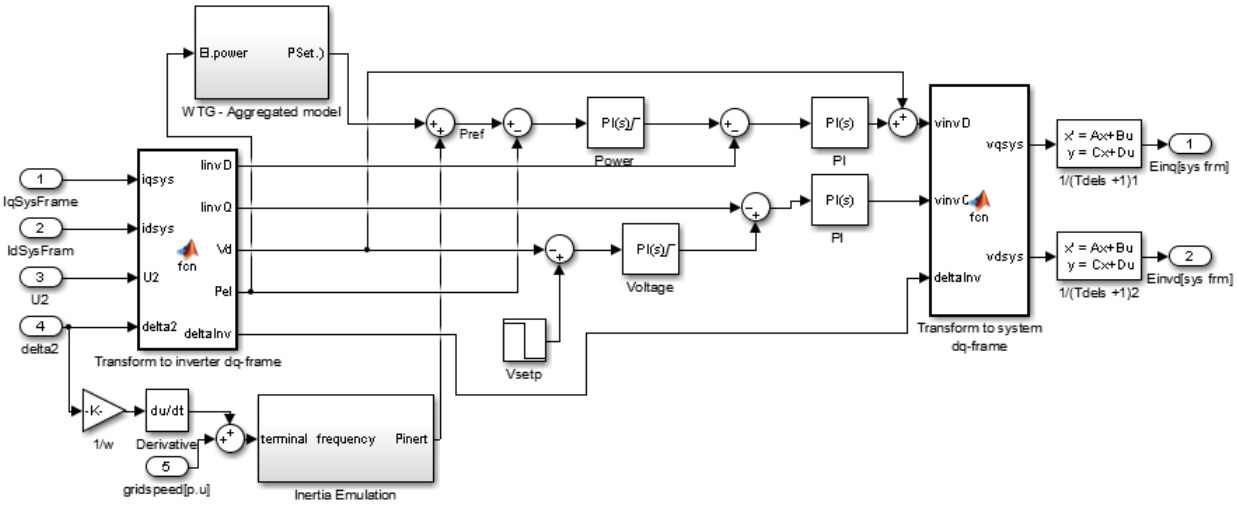

Figure 38: Inverter model

```
function [IinvD,IinvQ,Vd,Pel,deltaInv] = fcn(iqsys,idsys,U2,delta2)
xt = 0.07;
%Inverter voltage in system reference
Vinvsys = U2*cos(delta2)+1i*U2*sin(delta2)-idsys*xt+1i*iqsys*xt;

Vd = abs(Vinvsys);
d3= angle(Vinvsys);

%Currents in inverter reference frame. Inverter voltage is d-axis ref.
IinvD = iqsys*cos(d3)+idsys*sin(d3);
IinvQ = iqsys*sin(d3)-idsys*cos(d3);


Pel = Vd*IinvD;
%Q = -Vd*IinvQ;
deltaInv = d3;
end
```

Figure 39: Script: Transformation to inverter dq frame

```
function [vqsys,vdsys] = fcn(vinvD,vinvQ,deltaInv)

vqsys = vinvD*cos(deltaInv)+vinvQ*sin(deltaInv);
vdsys = vinvD*sin(deltaInv)-vinvQ*cos(deltaInv);

end
```

Figure 40: Script: Transformation to system dq-frame

Wind turbine model

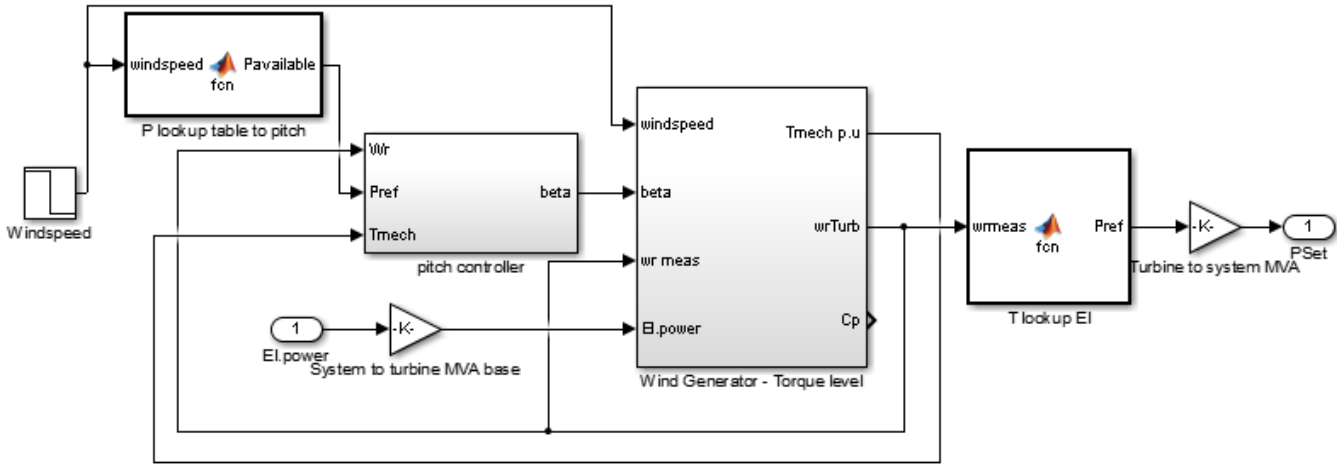

Figure 41: Top level of wind turbine model

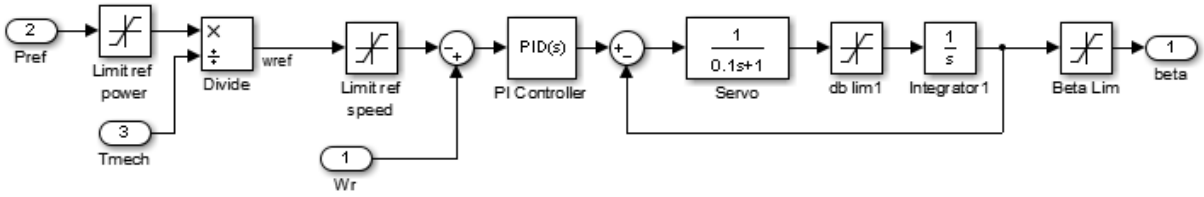

Figure 42: Pitch controller model

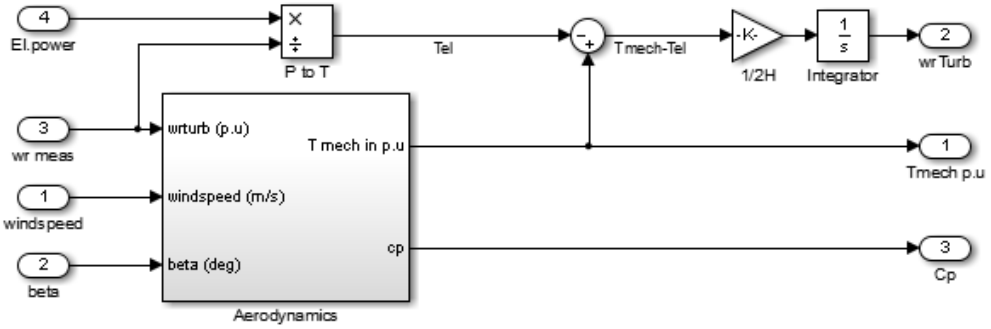

Figure 43: Torque level and swing equation in WTG.

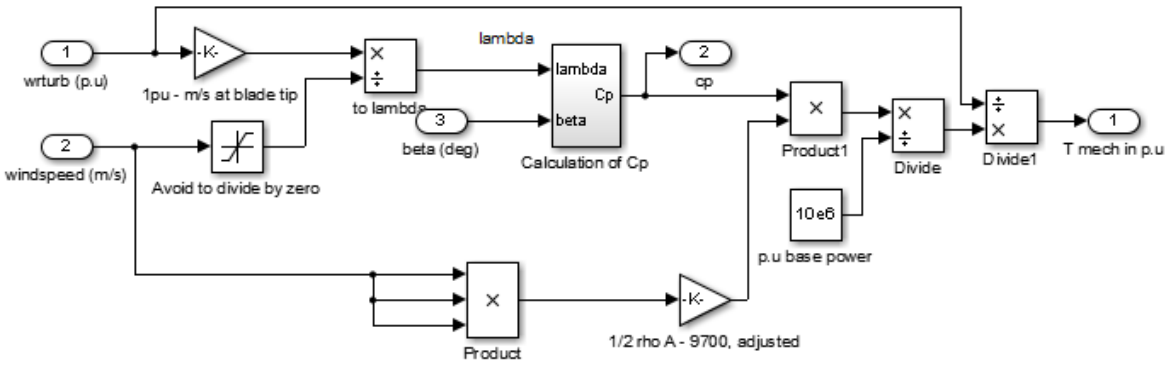

Figure 44: Aerodynamics in WTG model

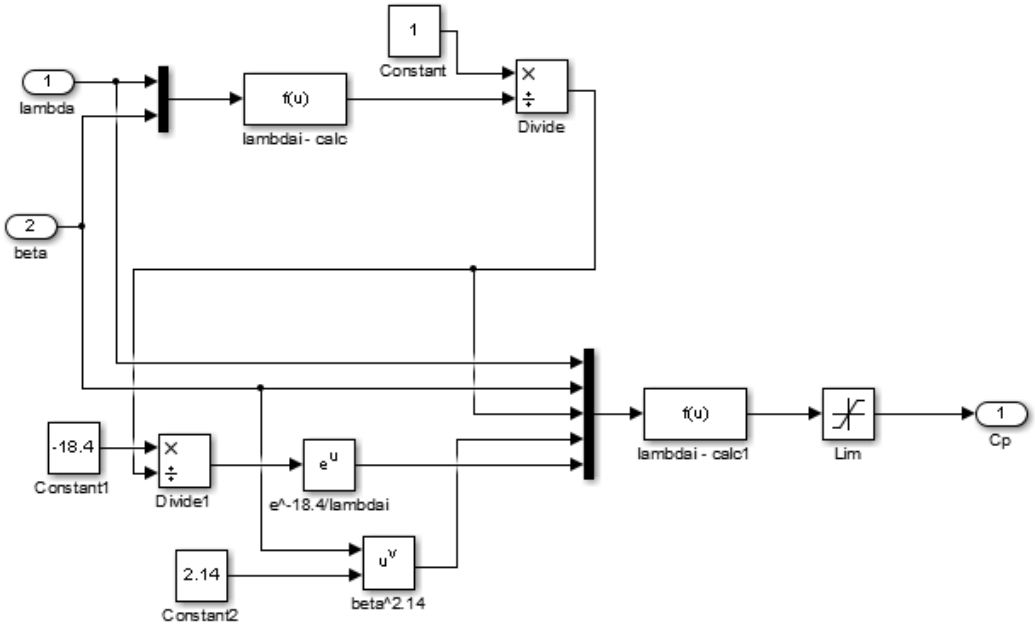

Figure 45: Numerical approximation to coefficient of performance.

References

[1] FIKS - Funksjonskrav i kraftsystemet 2012, Statnett

[2] Power system dynamics: stability ans control, J. Machowski, J.W. Bialek, J.R.Bumby, 2nd edition, 2008, John Wiley ans Sons, Ltd.

[3] D.Yuan,Z.Tian,S.Wang, "Mechanical and electrical design of the Three Gorges Project", Renewable Energy Landolt-Bornstein, Group VIII, Advanced Materials and Technologies, Volume 3C, 2006, pp 73-128

[4] "Power system operation and frequency control","Advanced Modelling of Synchronous Machines" and "Electromechanical dynamics - Small disturbances" , Kjetil Uhlen and Olav Bjarte Fosso, Dept. of Electrical Engineering, NTNU, Lectures in course TET4180 Power System Stability and Control.

[5] "Frequency support from doubly fed induction wind turbines", G.Ramtharan, J.B. Ekanayake and N.Jenkins, 2007.

[6] "Dynamic Modeling of Inverter-Based Distribution Generators with Voltage Positive Feedback Anti-Islanding protection",X. Wang, T.R Ricciardi, D. Salles, W. Freitas, IREP Symposium - Bulk Power Systems Dynamics and Control, Aug 2010.

[7] http://upload.wikimedia.org/wikipedia/commons/1/12/TypicalStateSpacemodel.png.

[8] "Active Power Controls from Wind Power: Bridging the Gaps", NREL/TP-5D00-60574, E.Ela, V.Gevorgian, P.Fleming, Y.C.Zhang, J.Aho, A.Buckspan, L.Pao, V.Singhvi, A.Tuohy, P.Pourbeik, D.Brooks. January 2014.

[9] Mohammad Seyedi, Math Bollen, "The utilization of syntethic inertia from wind farms and its impact on existing speed governors and system performance", Part 2 Report of Vindforsk Project V-369, Elforsk.

[10] "Temporary Rotor Inertial control of Wind Turbine to Support the Grid Frequency Regulation", Bing Liu, Kjetil Uhlen, Tore Undelad, Dep. of Electrical Power Engineering, NTNU, 9th Deep Sea Offshore Wind RnD Seminar, 19-20. jan, 2012.